THE ELECTRONIC BAND SYSTEMS OF $^{12}C^{16}O^{+}$

CENTRE FOR NEWFOUNDLAND STUDIES

TOTAL OF 10 PAGES ONLY
MAY BE XEROXED

(Without Author's Permission)

CHANDRAN HARIDASS

THE ELECTRONIC BAND SYSTEMS OF $^{12}C^{16}O^{+}$

BY

Chandran Haridass

A thesis submitted to the School of Graduate
Studies in partial fulfillment of the
requirements for the degree of
Master of Science

Department of Physics
Memorial University of Newfoundland
May 1990

St. John's Newfoundland

National Library of Canada
Bibliothèque nationale du Canada

Canadian Theses Service
Service des thèses canadiennes

Ottawa, Canada
K1A 0N4

The author has granted an irrevocable non-exclusive licence allowing the National Library of Canada to reproduce, loan, distribute or sell copies of his/her thesis by any means and in any form or format, making this thesis available to interested persons.

L'auteur a accordé une licence irrévocable et non exclusive permettant à la Bibliothèque nationale du Canada de reproduire, prêter, distribuer ou vendre des copies de sa thèse de quelque manière et sous quelque forme que ce soit pour mettre des exemplaires de cette thèse à la disposition des personnes intéressées.

The author retains ownership of the copyright in his/her thesis. Neither the thesis nor substantial extracts from it may be printed or otherwise reproduced without his/her permission.

L'auteur conserve la propriété du droit d'auteur qui protège sa thèse. Ni la thèse ni des extraits substantiels de celle-ci ne doivent être imprimés ou autrement reproduits sans son autorisation.

ISBN 0-315-68276-0

Canada

ACKNOWLEDGMENTS

I wish to express my grateful thanks to my supervisor, Professor S. P. Reddy, for his encouragement and guidance in the various stages of my research project and other academic pursuits.

My sincere appreciation to Dr. C. V. V. Prasad whose constructive and valuable criticism has helped in the improvement of this thesis.

I extend my thanks to the following technical personnel for their help in completing the research project: Messrs. T. G. White, M. Ryan, and W. Holly for the mechanical work; D. Seymour, M. Hatswell, and T. Perks for their skillful glass blowing; R. Guest for some drafting work; and R. Bradley for some photographic work. It is my pleasure to thank Mrs. Joy Simmons for her patient and skillful typing of the manuscript. I would like to thank Mr. Robin Kelly for his help in performing some computational work.

I thank the Memorial University of Newfoundland for providing financial support in the form of a Graduate Fellowship and Graduate Teaching Assistantships and bursary from Dr. Reddy's NSERC grant.

I am immensely indebted to Dr. N. Krishnamurthy, Madurai Kamaraj University, Madurai, India, who inspired me to undertake research in molecular spectroscopy.

ABSTRACT

The electronic band spectrum of the molecular ion $^{12}C^{15}O^{+}$ is of considerable importance to astrophysics as this species is one of the major constituent of the solar chromosphere, stellar atmospheres, and comet tails. It has also application in the study of radiative heating of hypersonic space craft at escape velocity and in the atmospheric fringe of the planet Venus.

The molecular ion CO^{+} was excited in a hollow-cathode discharge tube of special design (S. P. Reddy and C. V. V. Prasad, J. Phys. E. Sci. Instrum. 22, 306 (1989)). The comet-tail ($A^2\Pi_i$ - $X^2\Sigma^{+}$) band system of this molecular ion occurring in the cathode glow of the discharge tube was photographed in the spectral region 3345 - 8500 Å on a 2 m Bausch and Lomb dual-grating spectrograph in the first order of a 600 grooves/mm grating under medium resolution. Spectra were also recorded under high resolution on the same spectrograph in the second and third orders of a 1200 grooves/mm grating as well as on a 3.4 m Jarrell-Ash Ebert grating spectrograph in the second, third, and fourth orders of a 1200 grooves/mm grating. Of the seventeen bands with v' = 0 to 8 and v" = 0 to 4 recorded in this system, detailed rotational analysis of twelve (6-0, 4-0, 3-0, 2-0, 1-0, 2-1, 1-1, 0-1, 2-3, 0-2, 0-3, and 0-4) bands have been carried out. Rotational constants were obtained for the $A^2\Pi_i$ and $X^2\Sigma^{+}$ states using the effective Hamiltonian proposed by Brown and his co-workers (J. M. Brown et al., J. Mol. Spectrosc. 74, 294 (1979)).

Experimental data on the rotational structure of the first negative ($B^2\Sigma^+ - X^2\Sigma^+$) system (Rao, Astrophys. J. 111, 50 (1950) and Misra et al., J. Mol. Spectrosc. 125, 54 (1987)), the Baldet-Johnson ($B^2\Sigma^+ - A^2\Pi_i$) system (Jakubek et al., Can. J. Phys. 65, 94 (1987)), and the microwave spectrum of the v = 0 level (Sastry et al., Astrophys. J. 250, L91 (1981)) and of the v= 0, 1, and 2 levels (Bogey et al., J. Chem. Phys. 79, 4704 (1983)) of CO^+ have been reanalysed using the effective Hamiltonian. A single set of molecular constants were then obtained for the X, A, and B states of CO^+ by the method of a global fit of the molecular constants obtained from the analysis of the comet-tail, Baldet-Johnson and first negative systems and the microwave data. The vibrational constants for these three states were obtained from the band origin data.

CONTENTS

CHAPTER 1

INTRODUCTION

1.1 Significance of molecular spectra in atmospheric physics and astrophysics

The spectroscopic studies of the molecules progressed with the development of the quantum theory in the late 1920's. The electronic spectra of the molecules provide information about the vibration and rotation of their nuclei and their electronic structure. From the electronic structure, an insight into the important properties such as chemical valence can be achieved. From a detailed analysis of the electronic spectrum of a molecule, its electronic, vibrational, and rotational levels can be derived very precisely. From this, one can obtain information about its moment of inertia, internuclear separation, and nature of the coupling between the electronic and rotational motions of different electronic states. Intensities of the bands of the electronic spectra can be calculated from the vibrational and rotational constants of the electronic states and other molecular data. From the vibrational frequencies and the corresponding anharmonicities, forces between the atoms of a molecule and its dissociation energy can be estimated. Thermodynamic properties such as specific heat, entropy, and free energy can be estimated from the knowledge of the vibrational and rotational partition functions. Thus the study of the electronic spectra of a molecule enables one to understand its

various physical and chemical properties.

Molecular spectra also play a very important role in the atmospheric and astrophysical phenomena. Examples of these are the molecular absorption spectrum of the earth's atmosphere, the emission band spectra of the aurora, the radiation from the night sky and the twilight produced in the upper layers of the atmosphere, solar spectrum, cometary spectra, and spectrum of lightning etc. From the intensity distribution of the emission spectra of these celestial objects, their temperatures can be inferred. The presence of polyatomic molecules in the planetary atmospheres can be established from their absorption spectra. As an example of the application of molecular spectra to astrophysics the cometary spectra are briefly discussed here. Various parts of a typical comet are shown in Fig. 1. It consists of a coma that appears as a round and diffuse nebulous glow, a nucleus in the middle of the coma, and two tails. The gas atoms released from the nucleus by the radiation from the sun have a velocity of ~ 1 km/s. The nucleus has an approximate diameter of 1 to 10 km. The coma and the nucleus together constitute the head of the comet. One of the two tails, known as ion tail, is nearly straight and consists of molecular ions such as CO^+, N_2^+, and H_2O^+ etc. The other tail is known as dust tail as it consists of mostly dust particles. The frozen solid nucleus of the comet can be seen from the earth by the sunlight it reflects. The coma gives molecular emission from the radicals C_2, CN, OH, NH, and NH_2 etc., overlapped by a weak

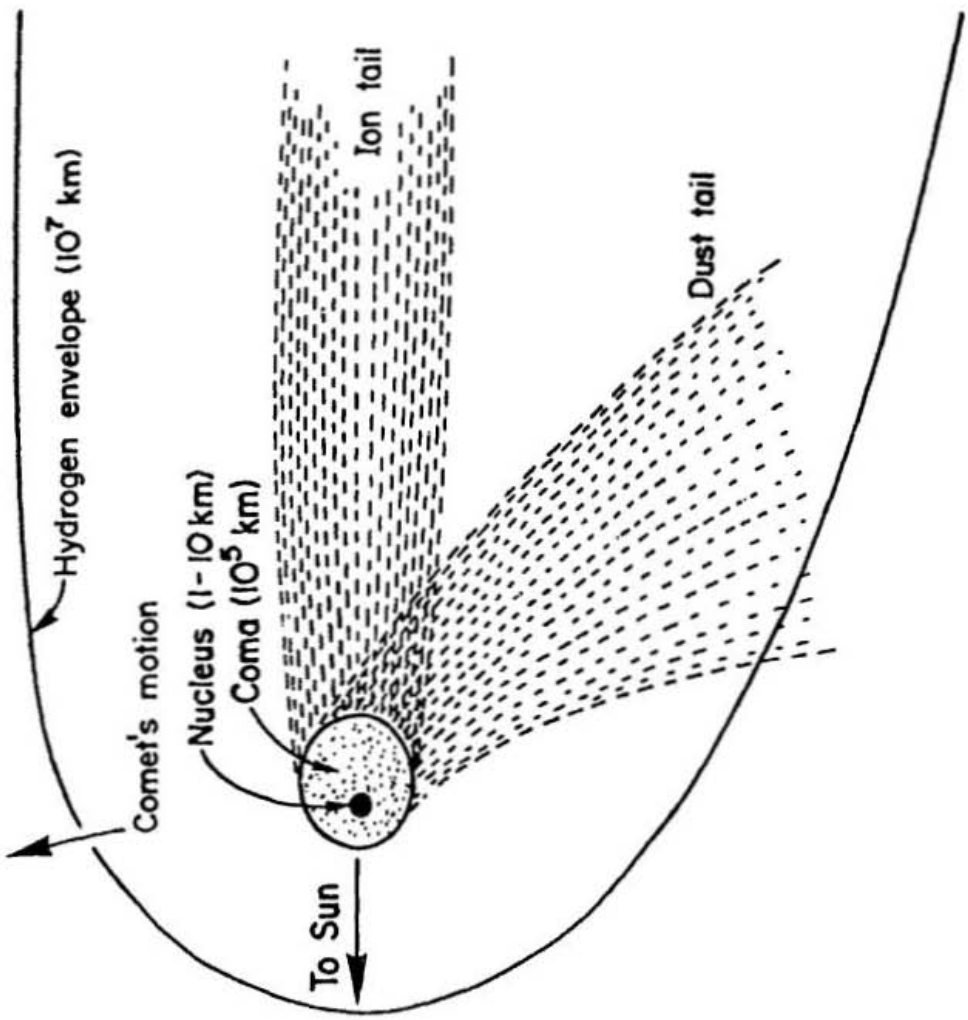

Figure 1. Parts of a typical comet.

continuum with Fraunhofer lines. When the comet is far away from the sun the parent molecules of the most abundant radicals are presumed to be H_2O, CH_4, and NH_3. It was found that for the band systems observed in comets the lower state is the ground state of the particular molecule. This suggests that these bands are excited by sunlight through a resonance fluorescence mechanism. This fluorescence mechanism is confirmed by a study of the intensity distribution in the rotational structure of the cometary bands. The partial molecular density in the comets is estimated from the total intensity of the bands (see for example, Wurm 1943, Herzberg 1950, and Abell 1975).

1.2 Electronic spectra of CO and CO^+

The neutral carbon monoxide CO and its ion CO^+ are important for a number of reasons including for their astrophysical significance. Carbon monoxide is present in solar chromosphere, stellar atmospheres, and tails of comets. Also, the comet-tail ($A^2\Pi_i - X^2\Sigma^+$) band system of CO^+ was first observed in the tail of the Comet Morehouse - 1908c by Pluvinel and Baldet (1909 and 1911) and was later observed in the laboratory by Fowler (1909 and 1910).

The type of the molecular binding and the nature of the electronic states of a molecule are determined by electrons in the outer most shells of the constituent atoms of the molecule. The electronic configurations of the ground states

of the carbon and oxygen atoms are

$$C: K\ 2s^2\ 2p^2; \quad O: K\ 2s^2\ 2p^4 \qquad [1.1]$$

The electronic configuration of the ground state ($X^1\Sigma^+$) of the CO molecule is written as (Mulliken 1932)

$$K\ K\ (z\sigma)^2\ (y\sigma)^2\ (w\pi)^4\ (x\sigma)^2 : X^1\Sigma^+ \qquad [1.2]$$

and those of the low lying excited states of CO are written by promoting one of the $x\sigma$ electrons to the $v\pi$ orbital and one of the $w\pi$ electrons to the $v\pi$ orbital. The resulting configurations are

$$---- (w\pi)^4\ (x\sigma)\ (v\pi) : a^3\Pi_r \text{ and } A^1\Pi, \qquad [1.3]$$

and

$$---- (w\pi)^3\ (x\sigma)^2\ (v\pi) : a'^3\Sigma^+,\ e^3\Sigma^-,\ d^3\Delta_i,\ ^1\Sigma^+,$$
$$I^1\Sigma^-, \text{ and } D^1\Delta. \qquad [1.4]$$

The $^1\Sigma^+$ state in Eq. [1.4] has not yet been observed. Higher excited states of CO are obtained by raising one of the $x\sigma$ electrons of Eq. [1.2] to the $w\sigma$ orbital and one of the $w\pi$ electrons to the $u\sigma$ orbitals as given below:

$$---- (w\pi)^4\ (x\upsilon)\ (u\sigma) : ^3\Sigma^+ \text{ and } ^1\Sigma^+, \qquad [1.5]$$

and

$$---- (w\pi)^3\ (x\sigma)^2\ (u\sigma) : ^3\Pi_i \text{ and } ^1\Pi. \qquad [1.6]$$

However, none of these four states has been observed so far. Further higher excited states of CO are obtained by promoting one of the $x\sigma$ electrons to the Rydberg orbitals $3s\sigma$, $3p\sigma$, and $3p\pi$ etc., which are identified as

$$---- (w\pi)^4\ (x\sigma)\ (3s\sigma) : b^3\Sigma^+ \text{ and } B^1\Sigma^+. \qquad [1.7]$$

$$----\ -\ -\ (3p\sigma) : j^3\Sigma^+ \text{ and } C^1\Sigma^+. \qquad [1.8]$$

$$----\ -\ -\ (3p\pi) : c^3\Pi_i \text{ and } E^1\Pi. \qquad [1.9]$$

These Rydberg states converge to the ground state ($X^2\Sigma^+$) of the CO^+ molecule (Lefebvre-Brian et al. 1964). The electronic spectrum of CO has been extensively studied both in emission and absorption in the spectral region 600 - 8600 Å. A total of 30 electronic transitions are observed from the 24 known electronic states of CO. Of these, the prominent band systems are (i) the Ångström ($B^1\Sigma^+ - A^1\Pi$) system (4100 - 6600 Å), (ii) the Herzberg ($C^1\Sigma^+ - A^1\Pi$) system (3680 - 5710 Å), (iii) the third positive ($b^3\Sigma^+ - a^3\Pi_r$) system (2600 - 3800 Å), and (iv) the fourth positive ($A^1\Pi - X^1\Sigma^+$) system (1140 - 2800 Å).

The electronic configurations of the ground ($X^2\Sigma^+$) and the first three excited states ($A^2\Pi_i$, $B^2\Sigma^+$, and $C^2\Delta_r$) of CO$^+$ are

$$KK\ (z\sigma)^2\ (y\sigma)^2\ (w\pi)^4\ (x\sigma) : X^2\Sigma^+, \qquad [1.10]$$

$$--\quad -\ (y\sigma)^2\ (w\pi)^3\ (x\sigma)^2 : A^2\Pi_i, \qquad [1.11]$$

$$--\quad -\ (y\sigma)\ (w\pi)^4\ (x\sigma)^2 : B^2\Sigma^+, \qquad [1.12]$$

and

$$--\quad -\ (y\sigma)^2\ (w\pi)^3\ (x\sigma)\ (v\pi) : C^2\Delta_r. \qquad [1.13]$$

The electronic states $X^2\Sigma^+$ and $A^2\Pi_i$ dissociate into $C^+(^2P)$ and $O(^3P)$ atoms whereas the $B^2\Sigma^+$ state dissociates into $C^+(^2P)$ and $O(^1D)$ atoms. The molecular states which are of present interest are $X^2\Sigma^+$, $A^2\Pi_i$, and $B^2\Sigma^+$ and their RKR potential energy curves along with that of the ground state ($X^1\Sigma^+$) of neutral CO are given in Fig. 2 (modified from Krupenie 1966).

For the CO^+ molecule, the X, A, and B states are clearly identified and the band system arising from these states are (i) the comet-tail ($A^2\Pi_i - X^2\Sigma^+$) system (3080 - 8500 Å), (ii) the Baldet-Johnson ($B^2\Sigma^+ - A^2\Pi_i$) system (3315 - 4236 Å), and

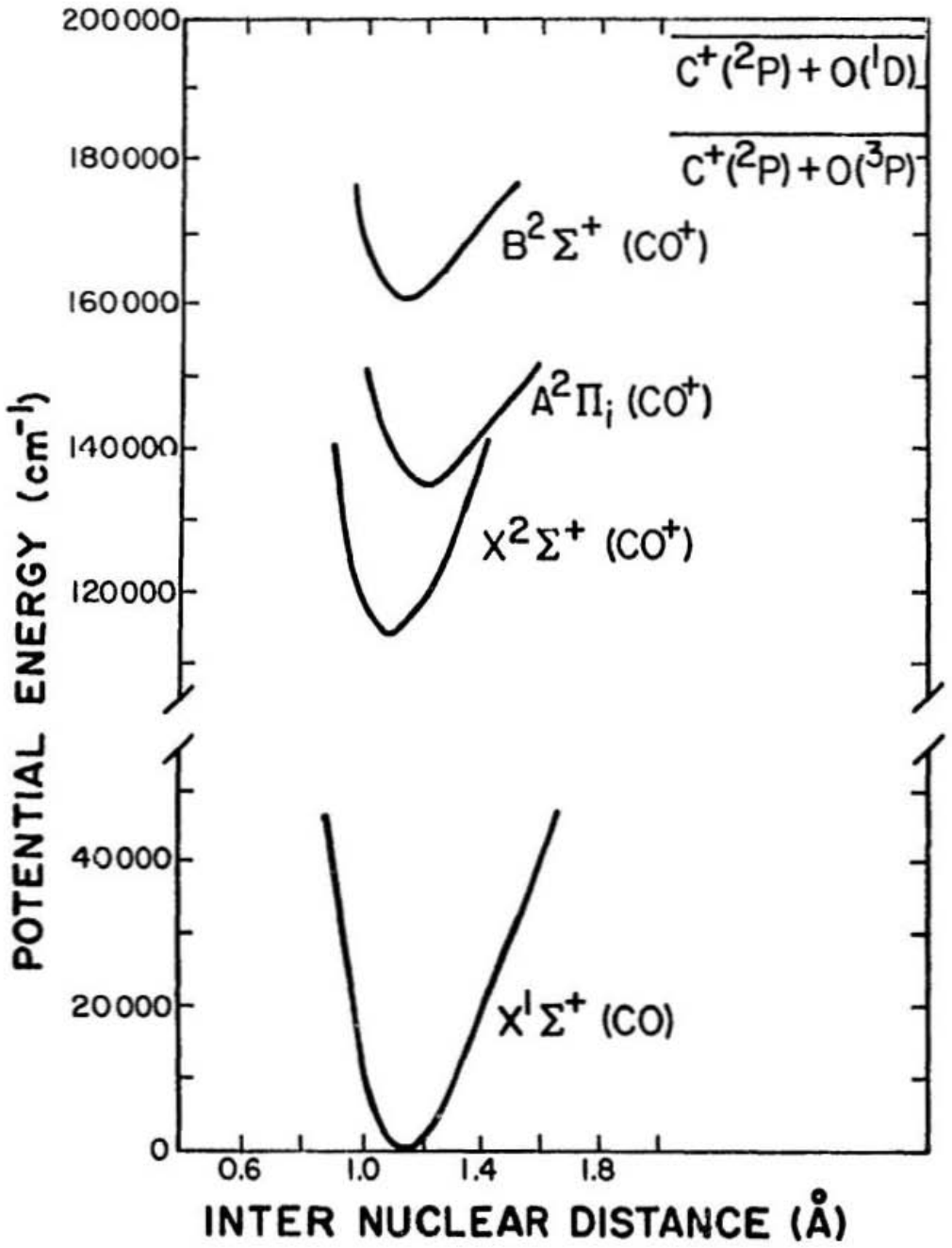

Figure 2. RKR potential energy curves for the ground state of CO and the X, A, and B states of CO^+.

(iii) the first negative ($B^2\Sigma^+ - X^2\Sigma^+$) system (1800 - 3102 Å). The transition $C^2\Delta_r - A^2\Pi_i$ in CO^+ was identified by Marchand et al. (1969), but its vibrational numbering is uncertain and the rotational structure is not completely resolved.

After the laboratory work of Fowler (1909 and 1910) several researchers also observed the bands of the comet-tail (A-X) system (see Krupenie 1966 and Huber and Herzberg 1979). Baldet (1925a,b) observed most of the known bands of this system and Birge (1925) identified the transition as ($A^2\Pi_r - X^2\Sigma^+$). Coster et al. (1932), Schmid and Gerö (1933), and Bulthuis (1935) performed the rotational analysis for several bands (v' = 2 to 11 and v'' = 0 to 2). Rao (1950a) did the rotational analysis of the 0-2, 0-3, and 0-4 bands of this system and identified the upper state as an inverted Π state and revised the vibrational assignments of this state by lowering the previous assignments by 3 units. These new assignments were later confirmed by Asundi et al. (1970) and Dhumwad et al. (1979) from the isotope shifts of the bands of the A-X system and the B-A system of $^{13}C^{16}O^+$ and $^{12}C^{18}O^+$, respectively, from the corresponding bands of $^{12}C^{16}O^+$. Gagnaire and Goure (1976) reanalysed the 2-0 band of this system of CO^+. Coxon and Foster (1982) carried out the deperturbation analysis of the v = 0, 5, and 10 levels of $A^2\Pi_i$ using the experimental data of Coster et al. (1932), Bulthuis (1935), and Rao (1950a). These authors found that the ground state rotational constants obtained by Gagnaire and Goure (1976) are

incorrect. Katayama and Welsh (1981) and Brown et al. (1984) reinvestigated the rotational structure of the 0-0 band. Vujisić and Pešić (1988) reinvestigated the 4-0, 3-0, and 0-2 bands of this system of $^{12}C^{16}O^{+}$. The previous work done on the rotational analysis of the comet-tail system since 1932 is summarized in Table 1.1.

The first negative ($B^2\Sigma^+ - X^2\Sigma^+$) system of CO^+ which consists of single-headed bands degraded to longer wavelengths was investigated by several researchers. Blackburn (1925) gave the first vibrational assignments for the bands of the system. Biskamp (1933) extended this system to shorter wavelengths and identified 22 additional bands under low dispersion in an intense high frequency discharge in helium containing a trace of CO. Coster et al. (1932) and Schmid (1932) performed the rotational analysis of a few bands of this system prior to Biskamp without providing reliable rotational constants. Schmid observed the splitting only in the spectral lines with high rotational quantum number (J = 30-34). Schmid and Gerö's work (1933) on the rotational analysis of the 0-0 band of this system established that the ground state is the common lower state of the comet-tail and first negative systems. The spin splitting in the $^2\Sigma$ states of CO^+ was first studied by Woods (1943). Rao (1950b) analyzed fifteen bands of this system rotationally and reported the rotational and vibrational constants for the X and B states along with the $|\gamma_v' - \gamma_v''|$ differences for some

TABLE 1.1 Rotational analysis of the comet-tail ($A^3\Pi_i - X^2\Sigma^+$) system of $^{12}C^{16}O^+$ prior to the present work

	Author	Band(s)	Remark(s)
1.	Coster et al. (1932)	5-0, 6-0, 7-0 8-0	$A^2\Pi$ was considered 'regular'. Rao (1950) identified State A as "inverted" and decreased the v' assignments by 3 units.
2.	Schmid & Gerö (1933)	3-0, 4-0, 4-1 5-1, 6-2, 7-2	Same remarks as above.
3.	Bulthuis (1935)	9-0, 10-0, 11-1 12-1, 13-1, 13-2 14-2	Same remarks as above.
4.	Rao (1950)	0-2, 0-3, 0-4	$A^2\Pi$ was identified as 'inverted'. v' assignments by Coster et al. (1932), Schmid and Gerö (1933), and Bulthuis (1935) were decreased by 3 units.
5.	Gagnaire & Goure (1976)	2-0	The band was not fully resolved and their calibration seemed to be erroneous as suspected by Coxon and Foster (1982).
6.	Katayama & Welsh (1981)	0-0	This band was excited by laser-induced fluorescence method; observed extra lines in the $^2\Pi_{1/2} - {}^2\Sigma^+$ sub-band; concluded that the extra lines were due to perturbations of A: v = 0 by X : v = 10.
7.	Coxon & Foster (1982)	5-0, 10-1, 10-2 0-2	No new experimental data. Depurturbation analysis was done for the data of the 5-0 (Coster et al. 1932: 8-0), 10-1, 10-2 (Bulthuis, 1935: 13-1, 13-2) and 0-2 (Rao, 1950) bands. Concluded that A, v = 0, 5 and 10 were perturbed.
8.	Brown et al. (1984)	0-0	Observed this band (also see Katayama and Welsh, 1981) in laser-induced fluorescence. Effective Hamiltonian technique was used for the upper level. These authors concluded that the data of Schmid and Gerö (1933) are questionable.
9.	Vujsić & Pešić (1988)	2-0, 3-0, 4-0	These are the 5-0, 6-0, and 7-0 bands reported by Coster et al. (1932). Molecular constants were determined, but effective Hamiltonian technique was not used.

bands. Rao's $|\gamma_v' - \gamma_v''|$ values are one half of those reported by Woods. For the previous work done on this system, the reader is referred to Krupenie (1966) and Huber and Herzberg (1979). Misra et al. (1987) reexamined the 0-0, 0-1, and 0-2 bands of the B-X system and reported the spin splitting constants for various vibrational levels by combining the earlier experimental data of Rao (1950b). Misra et al. included in their analysis the microwave data reported by Sastry et al. (1981) for $X^2\Sigma^+$, v = 0 and Bogey et al. (1982) for $X^2\Sigma^+$, v = 1.

The Baldet-Johnson ($B^2\Sigma^+ - A^2\Pi_i$) system consists of double double-headed bands degraded to shorter wavelengths. Baldet (1924) and Johnson (1925) were the first to investigate this system. Later Bulthuis (1934) gave the rotational analysis of the 0-0 and 0-1 bands. Rao and Sarma (1953) summarized the work on all three observed transitions for CO^+ stressing the revision of vibrational numbering for the A state. Conkić et al. (1978) reinvestigated the rotational structure of the 1-0 band of $^{12}C^{16}O^+$. Jakubek et al. (1987) photographed 0-0, 0-1, and 1-0 bands under high resolution and obtained precise values for the molecular constants of the $B^2\Sigma^+$, v = 0 and 1 and $A^2\Pi_i$, v = 0 and 1 states.

The CO^+ ion has a strong electric dipole moment and hence is expected to have a strong microwave spectrum. Dixon and Woods (1975) were the first to observe CO^+ terrestrially by microwave spectroscopy. In the laboratory, its millimeter

(Sastry et al. 1981 and Piltch et al. 1982) and submillimeter (Van den Heuvel et al. 1982) wave spectrum was measured in the ground vibrational state. Bogey et al. (1982) reported the observation of the rotational transition in the vibrational states v = 0 and 1. Subsequently Bogey et al. (1983) extended the measurements to higher vibrational levels of $^{12}C^{16}O^{+}$ and to other isotopomers (v ≤ 4 for $^{12}C^{16}O^{+}$, v = 0 and 1 for $^{12}C^{18}O^{+}$ and $^{13}C^{16}O^{+}$, and v = 0 for $^{13}C^{18}O^{+}$).

Considerable work on the rotational structure of the A-X, B-A, and B-X systems of the other isotopomers of CO^{+} has also been carried out. Recently in our laboratory the rotational analyses of the comet-tail band system (Prasad and Reddy, 1989), Baldet-Johnson system (Reddy and Prasad, 1989a) and the first negative system (Prasad and Reddy, 1990) of $^{13}C^{18}O^{+}$ were performed. For the references on the work done on the electronic band system of other isotopomers of CO^{+}, the reader is referred to these three papers. It may be mentioned that Brown et al. (1983) refitted the experimental data of the rotational structure of the (2-0) and (0-0) bands of the comet-tail system of $^{13}C^{16}O^{+}$, reported by Vujisic et al (1980) and concluded that the latter's work was erroneous.

1.3 Present investigation

The present work is concerned about the spectroscopy of the molecular ion $^{12}C^{16}O^{+}$. Prior to the present work several researchers investigated the A-X, B-X, and B-A systems of CO^{+}.

As far as the comet-tail system is concerned, even though 15 bands have been analyzed rotationally over a long period, the structure of several strong bands have not been analyzed. Analysis of the experimental data using the effective Hamiltonian of Brown et al. (1979) for $^2\Pi$ state is expected to give accurate molecular constants and none of the previous workers had the opportunity to use this method, except Brown et al. (1984) who analyzed the 0-0 band of the A-X system, excited by laser-induced fluorescence. As mentioned in the previous section all the recent studies on the comet-tail system were done on a few selected bands only (see Table 1.1) and hence it is considered essential to reinvestigate this important band system of CO^+ more exhaustively. In the present work the molecular ion $^{12}C^{16}O^+$ was excited in the cathode glow of a hollow discharge tube of special design (Reddy and Prasad 1989b). Seventeen bands with v' = 0 to 8 and v" = 0 to 4 of the comet-tail ($A^2\Pi_i$ - $X^2\Sigma^+$) system of this molecular ion occurring in the spectral region 3410 - 8480 Å were photographed under medium resolution. Of these, twelve bands (6-0, 4-0, 3-0, 2-0, 1-0, 2-1, 1-1, 0-1, 2-3, 0-2, 0-3, and 0-4) were photographed under higher resolution and their detailed rotational analysis has been carried out. The structure of six (6-0, 1-0, 2-1, 1-1, 0-1, and 2-3) of these twelve bands were analyzed for the first time since Rao (1950a) decreased the v' assignments by 3 units and correctly identified the A state as an inverted $^2\Pi$ state. Rotational constants were obtained for the $A^2\Pi_i$ and $X^2\Sigma^+$ states using the

effective Hamiltonians for the $^2\Pi$ (Brown et al. 1979) and $^2\Sigma^+$ states. The same method was used for the analysis of the experimental data of Jakubek et al. (1987) for the Baldet-Johnson ($B^2\Sigma^+ - A^2\Pi_i$) system. A similar method with an effective Hamiltonian of $^2\Sigma^+$ state was used for the analysis of the experimental data of Misra et al. (1987) and Rao (1950b) for the first negative ($B^2\Sigma^+ - X^2\Sigma^+$) system and the microwave data of Sastry et al. (1981) and Bogey et al. (1983) for the v = 0, 1, and 2 levels of the $X^2\Sigma^+$ state. The rotational constants of various vibrational levels and the band origins of several bands thus obtained from the band-by-band fits and from the microwave data were all merged together in step by step approach using a correlated least-squares method. A unique set of molecular constants for the $X^2\Sigma^+$, $A^2\Pi_i$, and $B^2\Sigma^+$ states, and the band origins of all the bands used in the analysis, of $^{12}C^{16}O^+$ were obtained from this global least-squares fit. Thus, this type of global fit combining all the available experimental data was attempted for the first time for the CO^+ ion. The present work provides statistically and spectroscopically more meaningful molecular constants for three electronic states of CO^+ which is important astrophysically. In Chapter 2, a description of the hollow cathode discharge tube and the details of the experimental techniques are presented. The method of analysis and the results obtained from the rotational analysis of the intense bands of the A-X system are given in Chapter 3. The procedure used for a global fit of all the available

experimental data and the final results are discussed in Chapter 4.

CHAPTER 2

EXPERIMENTAL TECHNIQUES

The spectrum of the molecular ion CO^+ was excited in the cathode column of a hollow-cathode discharge tube. Seventeen bands of the comet-tail ($A^2\Pi_i - X^2\Sigma^+$) system of this molecular ion were photographed under medium resolution. Of these, twelve bands were photographed under high resolution. The hollow-cathode discharge tube, two optical spectrographs used in the experimental work, and the experimental procedure are described in this chapter. A brief description of the mechanism of the hollow-cathode discharges and the measurement of the spectra are also included here.

2.1 The hollow-cathode discharge tube

The hollow-cathode discharge tube and the gas handling system are schematically shown in Fig. 3. The discharge tube consists of a hollow cathode (C) made from a copper cylinder 75 mm long, 17 mm in outer diameter and 1.5 mm in wall thickness. It was silver soldered (S) to a Kovar tube of a Kovar Pyrex seal (K), 19 mm in inner diameter. The Pyrex end of this seal was joined to the Pyrex glass body (P), 140 mm long and 46 mm in outer diameter. A side arm (A) 17 mm in outer diameter was attached to the main body. A tungsten anode (T) was fused into the branch of this side arm. Two S1-UV quartz windows W_1 and W_2, 1.5 mm thick, supplied by Esco Products Inc., were attached to the ground end surfaces of the

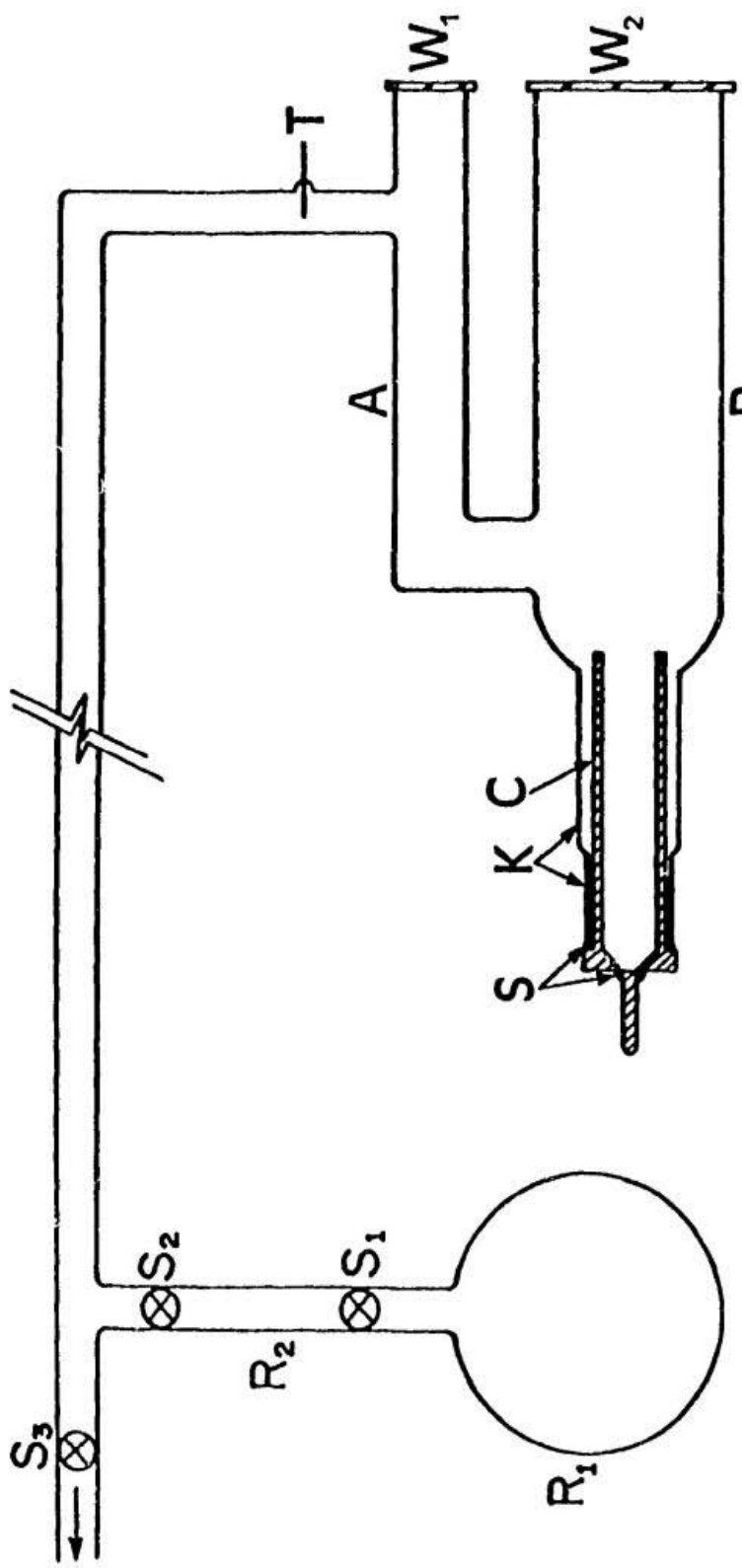

Figure 3. A schematic diagram of the hollow-cathode discharge tube and the associated gas handling system. R_1 and R_2 reservoirs; S_1, S_2 and S_3: stop cocks; S: silver soldering; K: Kovar-Pyrex seal; C: copper hollow-cathode; P: Pyrex glass body; A: anode branch; W_1 and W_2: quartz windows; and T: tungsten anode.

anode and cathode branches of the discharge tube, with Torr Seal, a low vapor pressure resin supplied by Varian Associates Inc. A ball and socket arrangement, which is not shown in Fig. 3, is provided to facilitate the connection or disconnection of the discharge tube to or from the pumping system.

In the present design the provision of separate columns for the anode and cathode facilitates photographing the two glows independently. The present design of the hollow-cathode discharge tube is somewhat similar to the one used by Herzberg et al. (1981) for the excitation of the spectra of triatomic molecules H_3 and D_3 in the cathode column which is immersed in liquid nitrogen. Inert gases like helium or neon can be used as a carrier gas to produce spectra of molecular ions or to suppress the spectra of neutral molecules. But for the production of the CO^+ emission no carrier gas was found to be necessary.

Reddy and Prasad (1989b) have demonstrated that in the modified hollow-cathode discharge tube the cathode glow is a rich source of positive molecular ions and the anode column consists exclusively of neutral molecules. Figure 4 illustrates the remarkable difference in the two spectra photographed from the anode and the cathode columns, respectively. The emission from anode column shown in Fig. 4(a) comprises of the 3A ($c^3\Sigma^+ - a^3\Pi_r$), the fourth positive ($A^1\Pi - X^1\Sigma^+$), and the third positive ($b^3\Sigma^+ - a^3\Pi_r$) systems of the neutral CO molecule with no trace of the CO^+ spectrum, while

Figure 4. Spectra excited in the hollow-cathode discharge tube with the CO gas in the spectral region 2100 - 3000 Å. (A) Spectrum of the anode column showing (a) the 3A ($c^3\Sigma^+ - a^3\Pi_r$) system, (b) the fourth positive ($A^1\Pi - X^1\Sigma^+$) system, and (d) the third positive ($b^3\Sigma^+ - a^3\Pi_r$) system of the neutral CO molecule. (B) Spectrum of the cathode glow showing (c) the first negative ($B^2\Sigma^+ - X^2\Sigma^+$) system of CO^+ and (e) the $A^2\Sigma_u^+ - X^2\Pi_{g,i}$ system of CO_2^+.

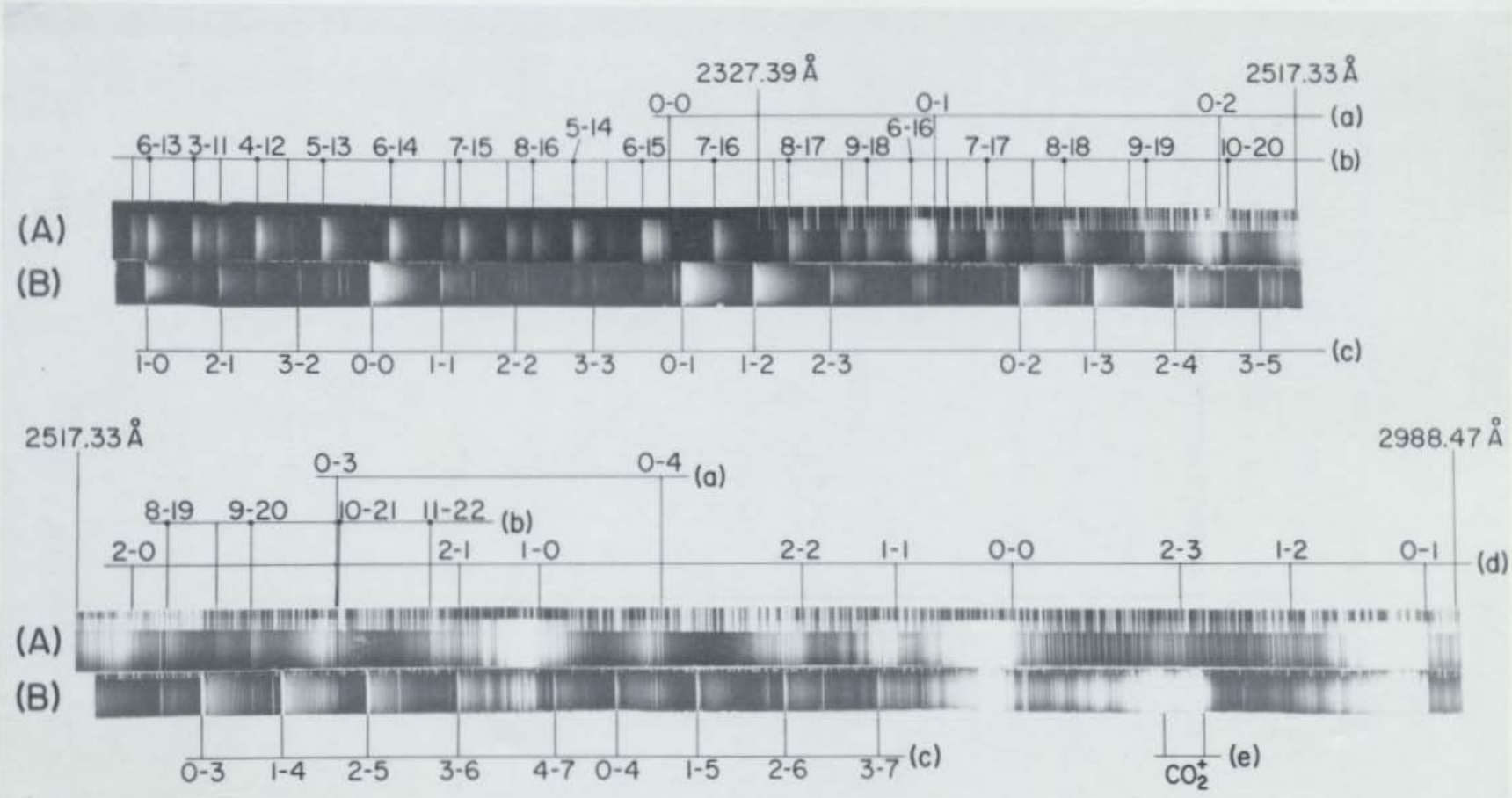
2327.39 Å
2517.33 Å
0-0
0-1
0-2
(a)
6-13 3-11 4-12 5-13 6-14 7-15 8-16 5-14 6-15 7-16 8-17 9-18 6-16 7-17 8-18 9-19 10-20
(b)
(A)
(B)
1-0 2-1 3-2 0-0 1-1 2-2 3-3 0-1 1-2 2-3 0-2 1-3 2-4 3-5
(c)
2517.33 Å
2988.47 Å
0-3
0-4
(a)
8-19 9-20 10-21 11-22
(b)
2-0 2-1 1-0 2-2 1-1 0-0 2-3 1-2 0-1
(d)
(A)
(B)
0-3 1-4 2-5 3-6 4-7 0-4 1-5 2-6 3-7
(c)
CO_2^+
(e)

spectrum of the cathode glow, shown in Fig. 4(b) consists of the first negative ($B^2\Sigma^+ - X^2\Sigma^+$) system of the molecular ion CO^+ and the two strong band heads of the $A^2\Sigma_u^+ - X^2\Pi_{g,i}$ system of CO_2^+. From Fig. 4, it is amply clear that two entirely different spectra can be obtained from the same discharge tube. The spectral broadenings such as Doppler broadening, pressure broadening, and Stark broadening are minimized in the hollow cathode discharges compared to the excitations in straight d.c. arcs and conventional electrodeless discharges.

An applied d.c. voltage of 1.1 kV from a power supply unit rated at 2 kV and 0.25 A was used to maintain the discharge in the hollow-cathode discharge tube. A detailed circuit diagram of this unit is shown in Fig. 5. The unit consists of a powerstat (P) which controls the primary voltage of the step-up transformer T. The output of the transformer was connected to a bridge rectifier through a resistor R_1 rated as 100 Ω, 100 W. The bridge rectifier consists of four high voltage diodes D_1 to D_4. The output from the rectifier was connected to the bleeder resistors R_3 to R_6 (DALE H100) each of which is rated at 20 kΩ, 100 W. The variable resistor R_2 acts as a bleeder resistor when it is set at 20 kΩ. The main function of the bleeder resistor is to quickly discharge the capacitor when the unit is switched off. The purpose of the resistor R_7 is to calibrate the voltmeter which measures the voltage across the resistor R_6 according to the voltage on the capacitor. The required voltage across the electrodes of the discharge tube was obtained by adjusting the powerstat.

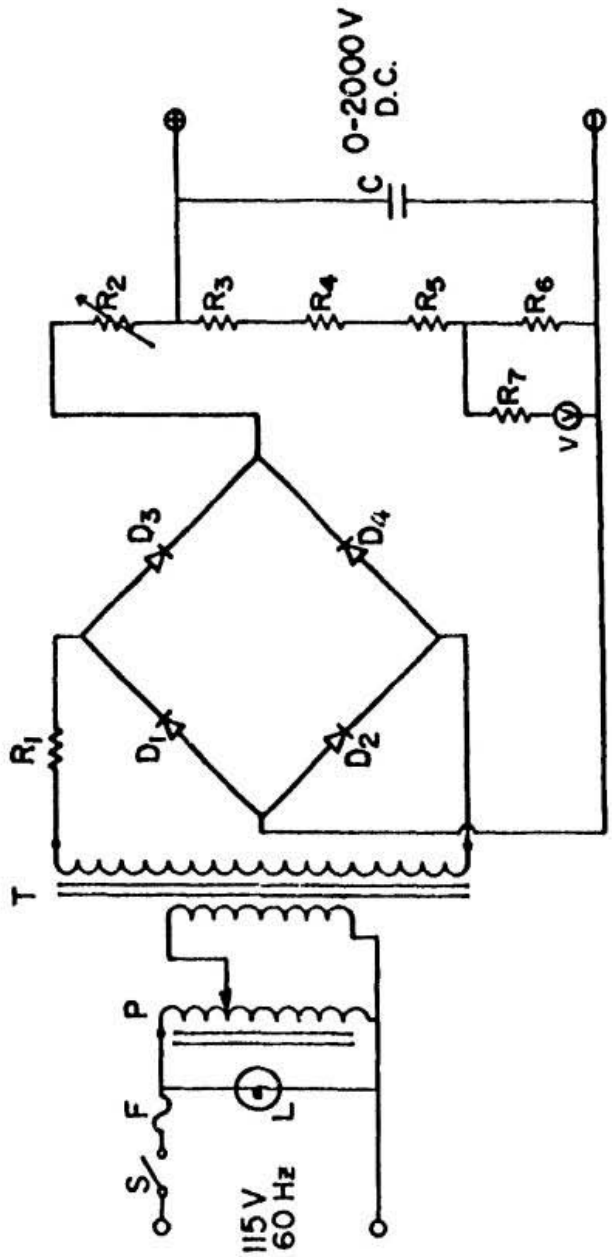

Figure 5. A schematic circuit diagram for the power supply unit. S: switch; F: fuse; L: indicator light; P: power-stat; T: step-up transformer; D_1-D_4: diodes; R_1, R_3-R_7: fixed resistors; R_2: variable resistor; V: voltmeter; and C: oil-filled capacitor.

The discharge was operated in the stationary condition of the gas. An applied d.c. voltage of 1100 V gave a current of 60 to 65 mA under normal operating conditions of the discharge tube. In the best operating conditions the pressure inside the discharge tube was found to be approximately 0.8 Torr as read on a thermocouple gauge.

2.2 Mechanism of hollow-cathode discharge

The emission of radiation in the hollow-cathode discharge tube is due to the collisions between the accelerated free electrons, released from the cathode because of the applied d.c. voltage between the electrodes, and the atoms or molecules of the experimental gas. In this collision process, the translational kinetic energy of the free electrons is transferred to the atoms or molecules, exciting them to different higher atomic states or rotational, vibrational, and electronic molecular states. Since these higher states of the atoms and molecules are unstable, they return to the lower energy states through the emission of electromagnetic radiation of energy $h\nu'$, h being the Planck's constant and ν' being the frequency in s^{-1}. The energy $h\nu'$ is equal to the energy difference between the upper and lower states. The emission of radiation is maintained continuously as long as the discharge tube is subjected to the electric field.

In the collision process some of the free electrons released from the cathode acquire sufficient kinetic energy

and ionize the molecules. These positive molecular ions concentrate around the cathode and the excited neutral molecules spread out into the anode branch of the discharge tube. This proposition is very clear from Fig. 4 where the cathode glow shows the spectrum of the CO^+ ion and the anode glow shows that of the neutral CO molecule.

2.3 Spectrographs

The emission spectrum of CO^+ from the cathode glow was photographed on a 2 m Bausch and Lomb (B&L) dual grating spectrograph and a 3.4 m Jarrell-Ash (J-A) Ebert grating spectrograph. These two spectrographs are briefly described in this section.

(i) The 2 m Bausch and Lomb dual grating spectrograph

A schematic representation of the optical layout of this spectrograph is shown in Fig. 6. A variable slit S allows the light from a source to enter the spectrograph. The light is then reflected by a plane mirror M onto the upper portion of a spherical mirror (SM), which has a focal length of 2 m and a numerical aperture of f/15.5. The advantage of this spectrograph is that it has two gratings mounted back to back on a rotatable turret T. The required grating (G_1 or G_2), either the one with 600 grooves/mm blazed at 2.5 μm or the one with 1200 grooves/mm blazed at 1.0 μm, each having a ruled area of 10.2 cm x 12.8 cm, can be selected by rotating the turret.

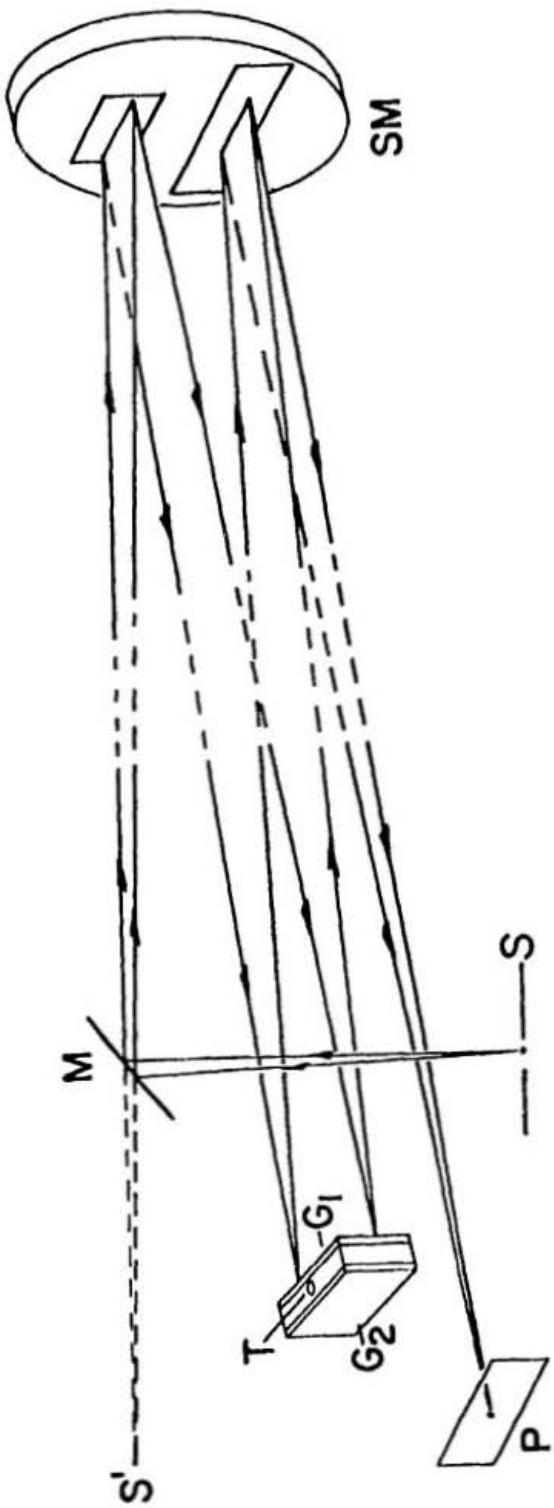

Figure 6. Optical layout of the 2 m Bausch and Lomb spectrograph. S: slit; M: plane mirror; P: photographic plate; T: rotatable turret; G_1 and G_2: gratings; and SM: spherical mirror. Here a monochromatic light beam is shown.

The collimated light from the spherical mirror is dispersed by the selected grating. The dispersed light from the grating is then incident on the lower section of the spherical mirror, which focuses it onto the photographic plate (P). The plate holder accommodates one plate of size 10.16 cm x 25.40 cm or two plates each of size 5.08 cm x 25.40 cm. The Hartman diaphragm located in front of the slit on the spectrograph enables the spectra to be photographed in juxtaposition. The measured reciprocal dispersions of the spectra photographed on the B&L spectrograph are 8.3 Å/mm at 5000 Å in the first order of the 600 grooves/mm grating and 1.05 Å/mm at 7200 Å in the second order of the 1200 grooves/mm grating.

(ii) <u>The 3.4 m Jarrell-Ash Ebert grating spectrograph</u>

The optical layout of this spectrograph is almost the same as that of the B&L spectrograph, except that the slit and the plate holder are on the same side of the spectrograph. In this instrument light from the source is incident directly on the upper section of the concave mirror after passing through two quartz cylindrical lenses (one collimating lens 10.0 cm in focal length and 3.0 cm in diameter and the other a condensing lens 45.0 cm in focal length and 3.0 cm in diameter). The concave mirror, which has a radius of curvature of 6.655 m, a diameter of 40.6 cm and a numerical aperture of f/35, collimates the light onto the grating. The dispersed light from the grating is focused onto the photographic plate by the lower section of the concave mirror. Best focus for a fixed

slit position is obtained by tilting the plate holder about the vertical axis. This tilt is found to have a linear dependence on the grating angle. A B&L plane grating having 1200 grooves/mm blazed at 1.4 μm and an MIT echelle grating having 300 grooves/mm blazed at 5.7 μm are available for this spectrograph. Both these gratings have a ruled width of 186 mm and a groove length of 63 mm. In the present work the 1200 grooves/mm grating was used in the second, third, and fourth orders. The measured reciprocal dispersions of the spectra are 0.34 Å/mm at 3450 Å in the fourth order and 0.98 Å/mm at 5100 Å in the second order.

2.4 Experimental procedure

The carbon monoxide gas whose purity is given as 99.99% was supplied by Matheson Gas products. The gas-handling system made of Pyrex glass which was attached to the hollow-cathode discharge tube is shown in Fig. 3. The discharge tube and the secondary reservoir R_2 were thoroughly evacuated. First, a small quantity of CO from the primary reservoir R_1 was admitted into R_2 by opening the stop cock S_1. The stop cock S_3 was closed and the gas was admitted into the discharge tube through stop cock S_2. A d.c. voltage of 1100 V was applied between the electrodes of the discharge tube and the discharge was initiated using a Tesla coil. Under normal operating conditions, the pressure inside the discharge tube was monitored to be approximately 0.8 Torr as read on a

thermocouple gauge. The emission spectra of CO^+ in the region 3000 - 8000 Å was photographed under medium dispersion on the B&L spectrograph and under high resolution on this spectrograph as well as on the J-A spectrograph. The slit width was maintained at 20 μm for the former and 30 μm for the latter. An Fe-Ne hollow-cathode lamp was used as a source for the standard spectrum. The details of the twelve bands photographed under high resolution are given in Table 2.1. Kodak SWR, Spectrum Analysis No. 1, 103 a-O, 103-F, and 1-N plates were used to photograph the spectrum in different spectral regions. Overlapping orders of the spectra were eliminated by using Corning and Hoya glass filters. Exposure times varied from 1 min to 12 h depending on the intensity of the band, sensitivity of the photographic plates, and the transmittance of the filters. The photographic plates were developed in Kodak developer D-19 at room temperature for about 4 minutes and were then fixed in Kodak fixer.

2.5 Measurement of spectra

A linear comparator, model M 1205C, supplied by the Gaertner Optical Company, Chicago, was used to measure the photographic plates. Although the least count of the instrument is 0.001 mm, the readings can be estimated to an accuracy of 0.0005 mm. The relation between the air wavelengths (λ_{air}) of the spectral lines and their comparator readings (d) is given by the formula

TABLE 2.1 Comet-tail bands of CO^+: recording details

Band	Spectrograph	Grating	Order
6-0	J-A	1200ℓ/mm (186 mm x 63 mm)	Fourth
4-0	J-A	"	Third
3-0	J-A	"	Third
2-0	J-A	"	Third
1-0	J-A	"	Third
2-1	J-A	"	Third
1-1	J-A	"	Second
0-2	J-A	"	Second
0-1	B&L	1200ℓ/mm (128 mm x 102 mm)	Second
2-3	B&L	"	Second
0-3	B&L	"	Second
0-4	B&L	600ℓ/mm (128 mm x 102 mm)	Third

$$\lambda_{air} = \sum_{i=0} a_i (d-d_0)^i, \qquad [2.1]$$

where d_0 is the comparator reading of the first standard line. The comparator readings (d) were obtained for the band heads, rotational lines, and standard Fe-Ne lines. The coefficients a_0, a_1, a_2, ... etc., were obtained using the method of least-squares by fitting the air wavelengths λ_{air} of the standard Fe-Ne lines and their corresponding comparator readings to Eq. [2.1]. In most of the cases a second degree polynomial fit was found to be adequate. The wavelengths of the standard Fe-Ne lines were taken from Crosswhite (1958 and 1975). In general the standard deviations of the fit were found to be around 0.03 Å and 0.003 Å for the medium and high resolution spectra, respectively. The air wavelengths of the band heads and the rotational lines were calculated from Eq. [2.1] after determining the coefficients. They were then converted into vacuum wavenumbers ν (cm^{-1}) by using Edlen's formula (1953) for the refractive index n of air,

$$n = 1 + 6432.8 \times 10^{-8} + \frac{2949810}{146 \times 10^8 - \nu^2} + \frac{25540}{41 \times 10^8 - \nu^2}, \qquad [2.2]$$

where $\nu = \frac{10^8}{n \times \lambda_{air}}$, ($\lambda_{air}$ in units of Ångströms).

An iterative method was employed to calculate the vacuum wavenumbers and the iteration was continued until the absolute value of the difference between the successive values of the wavenumbers was less than or equal to $10^{-10} cm^{-1}$. A VAX 11/785 computer was used to perform the numerical calculations.

CHAPTER 3

COMET-TAIL ($A^2\Pi_i - X^2\Sigma^+$) SYSTEM OF $^{12}C^{16}O^+$

3.1 Vibrational and rotational structure of an electronic band system

(i) Electronic and vibrational terms

Within the Born-Oppenheimer approximation, the total energy E (usually expressed in ergs) of a diatomic molecule (with the exclusion of the translational and nuclear spin energies) can be represented as the sum of its electronic energy E_e, vibrational energy E_v, and rotational energy E_r. Thus

$$E = E_e + E_v + E_r. \qquad [3.1]$$

The term value T (in cm^{-1}) of an energy level is given by

$$T = T_e + G(v) + F_v(J), \qquad [3.2]$$

where v and J are the vibrational and rotational quantum numbers, respectively, and T_e, G(v), and $F_v(J)$ are the electronic, vibrational and rotational terms respectively.

The electronic terms of different multiplet components are generally expressed in the first approximation (i.e., considering the case of zero rotation) as

$$T_e = T_0 + A\Lambda\Sigma_s, \qquad [3.3]$$

where T_0 is the electronic term, Λ and Σ_s are the quantized projections along the internuclear axis, of the electron orbital angular momentum L, and the electron spin angular momentum S, respectively, and A is the spin-orbit coupling

constant for the given electronic multiplet state. The electronic states are designated as Σ, Π, Δ, Φ, --- corresponding to Λ = 0, 1, 2, 3, ..., respectively. The quantity A is positive or negative depending on whether the state is regular or inverted. The electronic states $\Sigma(\Lambda = 0)$ are designated as Σ^+ or Σ^-, depending on whether the electronic wave function ψ_e remains unchanged or changes sign upon reflection at a plane passing through the internuclear axis. The multiplicity of an electronic state is given by 2S + 1, which is the number of Σ_s components along the internuclear axis. For example $S(\Sigma_s = 0)$ is zero for all singlet electronic states.

The vibrational terms G(v) of an electronic state of a molecule are expressed as

$$G(v) = \omega_e(v+1/2) - \omega_e x_e(v+1/2)^2 + \omega_e y_e(v+1/2)^3 + \ldots, \qquad [3.4]$$

where ω_e is the vibrational frequency and $\omega_e x_e$, $\omega_e y_e$, etc. are the anharmonic terms of the vibrational motion. The wavenumber (in cm^{-1}) of a spectral line arising from a transition between the vibrational levels neglecting the contribution from the rotational levels is given by

$$\nu_{v'v''} = \nu_e + \omega'_e(v'+1/2) - \omega'_e x'_e(v'+1/2)^2 + \omega'_e y'_e(v'+1/2)^3 + \ldots$$
$$- \omega''_e(v''+1/2) + \omega''_e x''_e(v''+1/2)^2 - \omega''_e y''_e(v''+1/2)^3 + \ldots \qquad [3.5]$$

The constants ν_e, ω_e, $\omega_e x_e$, $\omega_e y_e$, ..., etc., can be obtained either from a detailed rotational analysis of the band

structure or directly from the measured wavenumbers of the band heads. Equation [3.5] can be written in a simplified matrix form as

$$\mathbf{Y} = \mathbf{X}\beta + \delta \qquad [3.6]$$

where Y is a column vector containing either the values of the band origins (determined from the rotational analysis) or the vacuum wavenumbers of measured band heads as the input parameters and β is a column vector containing molecular constants to be estimated as output parameters. The coefficient matrix X contains the coefficients of ν_e, ω_e, $\omega_e X_e$, $\omega_e Y_e$, ..., etc., and δ is a column vector containing the unknown errors of measurements. The method of least-squares is used to obtain the molecular constants β which is given by

$$\hat{\beta} = (\mathbf{X}^T\mathbf{X})^{-1}\,\mathbf{X}^T\mathbf{Y} \qquad [3.7]$$

(where $\hat{}$ on β indicates that β is an estimate obtained from the least-squares fit). The estimated variance of the least-squares fit is given by

$$\hat{\sigma}^2 = (\mathbf{Y} - \mathbf{X}\beta)^T\,(\mathbf{Y} - \mathbf{X}\beta)/f \qquad [3.8]$$

where f is the number of degrees of freedom. The dispersion matrix $\hat{\mathbf{V}}$ is given by

$$\hat{\mathbf{V}} = (\mathbf{X}^T\mathbf{X})^{-1} \qquad [3.9]$$

and the variance-covariance matrix associated with $\hat{\beta}$ is given by

$$\hat{\theta} = \hat{\sigma}^2\hat{\mathbf{V}}. \qquad [3.10]$$

The uncertainties in the estimated values of the molecular constants are the square roots of the diagonal elements of $\hat{\theta}$.

(ii) Rotational terms of singlet electronic states

The rotational terms of a given vibrational level of a singlet electronic state are represented by

$$F_v(J) = B_v[J(J+1) - \Lambda^2] - D_v[J(J+1) - \Lambda^2]^2 + \ldots, \quad [3.11]$$

where $B_v = (h/8\pi^2 c\mu)\overline{(1/r_v^2)}$ is the rotational constant, μ and r_v being the reduced mass and the internuclear distance respectively of the molecule and $D_v = 4B_v^3/\omega^2$ is the centrifugal distortion constant. The constants B_v and D_v can be expressed in terms of the vibrational quantum number v and the equilibrium molecular constants as

$$B_v = B_e - \alpha_e (v + 1/2) + \gamma_e (v + 1/2)^2 + \ldots, \quad [3.12]$$

and

$$D_v = D_e + \beta_e (v + 1/2) + \ldots, \quad [3.13]$$

where

$$B_e = h/8\pi^2 c\mu r_e^2 \text{ and } D_e = 4B_e^3/\omega_e^2. \quad [3.14]$$

Here $\alpha_e << B_e$, $\gamma_e << \alpha_e$ and $\beta_e << D_e$. In the present work, the constants γ_e and β_e could not be estimated because of their very small magnitudes.

(iii) Coupling between rotation and electronic motion

Spin-orbit coupling: The interaction of the spin angular momentum of the electrons with their orbital angular momentum (usually known as spin-orbit coupling) causes splitting in the electronic states. There is no spin-orbit coupling for $^2\Sigma$, $^3\Sigma$, ..., etc., states. But states such as $^2\Pi$, $^3\Pi$, ..., $^2\Delta$, $^3\Delta$, ..., are split into 2S+1 components, which are distinguished

by the quantum number Σ_s which takes values S, S-1, ..., -S and represents the component of the spin angular momentum along the internuclear axis. The resultant of the electronic orbital and spin angular momenta in the direction of the internuclear axis, represented by the quantum number Ω is given by

$$\Omega = \Lambda + \Sigma_s. \qquad [3.15]$$

The value of Ω is indicated as a subscript following the term symbol. Thus the components arising from the spin-orbit coupling of a $^2\Pi$ state are $^2\Pi_{3/2}$ and $^2\Pi_{1/2}$. If the rotational angular momentum R of the molecule is imposed on the spin splitting, we come across several coupling cases, which are classified into five cases by Hund and are known as Hund's coupling cases. Of these five, Hund's case (a) and case (b) are important for the present work.

In Hund's case (a), R and Ω combine to form the total angular momentum J. For a given value of the quantum number Ω, J has the values

$$J = \Omega, \ \Omega + 1, \ \Omega + 2, \ \ldots \qquad [3.16]$$

Both J and Ω have either integer or half integer values depending on whether the multiplicity of the state is odd or even, respectively.

<u>Λ-type doubling</u>: The coupling between the rotation of the molecule and the orbital motion of its electrons is very small. However, this gives a splitting of the degeneracy that arises for electronic states with $\Lambda \neq 0$. This splitting is called Λ-type doubling. The split levels are either positive

(+) or negative (-) corresponding to the positive and negative eigen functions that correspond to the orbital motion of the electrons around the internuclear axis. This positive and negative character of the rotational levels is known as parity.

Hund's case (b) arises when the spin vector **S** is very weakly coupled to the internuclear axis as a consequence of its coupling with the axis of rotation of the molecule. Such a situation applies to Σ states almost always; it also applies to Π, Δ, ... states for small atomic numbers. In Hund's case (b) Ω is not defined. The component of **L** along the internuclear axis, i.e., Λ, combines with **R** to form the new vector **N**, which is the total angular momentum apart from the spin. The possible values of the quantum number N are

$$N = \Lambda, \Lambda + 1, \Lambda + 2, \ldots \qquad [3.17]$$

If $\Lambda = 0$, N takes all integer values from zero onward. The vector **N** combines with **S** to form **J**. For a given N, J has the values

$$J = N + S, N + S - 1, \ldots |N - S|. \qquad [3.18]$$

Thus each rotational level N has (2S+1) components which represent the multiplicity of the states. Kopp and Hougen (1967) introduced the following convention for labelling the rotational levels with half integer J values:

'Levels with parity $[+(-1)^{J-1/2}]$ are e levels and those with parity $[-(-1)^{J-1/2}]$ are f levels.'

Later Brown et al. (1975) extended this labelling convention to the rotational levels with integral J values which is

stated as follows:

'Levels with parity $[+(-1)^J]$ are e levels, and those with parity $[-(-1)^J]$ are f levels.'

3.2 Method of rotational analysis

(i) Effective Hamiltonian

The effective Hamiltonian for a diatomic molecule in the absence of external magnetic or electric field is given by

$$H = H_0 + H_{rot} + H_{cd} + H_{fs} + H_{hfs}, \qquad [3.19]$$

where H_0 includes the terms which are independent of rotation and represents the vibronic term energy T_v for the allowed vibrational states of the different electronic states. The term H_{rot} represents the Hamiltonian describing the rotation of the nuclei, and is given by

$$H_{rot} = B(r)\ \mathbf{R}^2 \qquad [3.20]$$

$$= (h/8\pi^2\mu r^2)\ (\mathbf{J}-\mathbf{L}-\mathbf{S})^2, \qquad [3.20a]$$

where B(r) is the radial part of the rotational energy operator, μ is the reduced mass, r is the internuclear distance, and R is the rotational angular momentum operator. The term H_{cd} in Eq. [3.19] represents the Hamiltonian for the centrifugal distortion and is given by

$$H_{cd} = -D(R^2)^2 + H(R^2)^3 + \ldots, \qquad [3.21]$$

where D and H are the quartic and sextic distortion constants. The third term H_{fs} in Eq. [3.19] describes the fine structure

of spectral levels and is composed of four parts. It is written as

$$H_{fs} = H_{so} + H_{ss} + H_{sr} + H_{ld}, \qquad [3.22]$$

where H_{so} represents the spin-orbit interaction and can be written as

$$H_{so} = A(r)\ \mathbf{L} \cdot \mathbf{S} + \text{----} \qquad [3.22a]$$

$$= A(r)\ (L_zS_z + 1/2\ L_+S_- + 1/2\ L_-S_+) + \text{----}. \qquad [3.22b]$$

where A(r) is the spin-orbit coupling constant. Equations [3.22 a & b] also contain additional terms involving the centrifugal corrections to the constant A, i.e., terms with A_{Dv}, A_{Hv}, A_{Lv}, etc. The term H_{ss} in Eq. [3.22] represents the spin-spin interaction term and is zero for all doublet states as shown below. The term H_{ss} can be represented as

$$H_{ss} = \epsilon(r)\ (3S_z^2 - S^2). \qquad [3.22c]$$

The matrix element for S_z is Σ_s and for doublet states it takes values + 1/2 & -1/2, and that of S^2 is written as S(S+1) and is equal to 3/4. With the help of the matrix elements Σ_s and S(S+1) it can be easily verified that the expression $[3\Sigma_s^2 - S(S+1)]$ is always equal to zero for the doublet states. The term H_{sr} in Eq. [3.22] is the spin-rotation Hamiltonian and is given by

$$H_{sr} = \gamma(r)\ \mathbf{R} \cdot \mathbf{S} \qquad [3.22d]$$

$$= \gamma(r)\ (\mathbf{J}-\mathbf{L}-\mathbf{S}) \cdot \mathbf{S}, \qquad [3.22e]$$

where $\gamma(r)$ is the spin-rotation constant. The last term H_{ld} in Eq. [3.22] represents the Λ-doubling in rotational levels and contains the terms with the Λ-doubling parameters o, p, q, and their centrifugal corrections. This Hamiltonian can be expressed as

$$H_{ld} = o(r)\ (\Lambda_+^2 S_-^2 + \Lambda_-^2 S_+^2) + p(r)\ (\Lambda_+^2 S_- N_- + \Lambda_-^2 S_+ N_+) - q(r)\ (\Lambda_+^2 N_-^2 + \Lambda_-^2 N_+^2) + \ldots \qquad [3.22f]$$

The Λ-doubling parameter o(r) in this expression has non-zero value only for the states with multiplicity three and higher. Only the parameters p(r) and q(r) and in some cases their centrifugal corrections are significant for the $^2\Pi$ states. The last term H_{hfs} in Eq. [3.19] represents the Hamiltonian for the hyperfine structure, which is rarely resolved in the optical spectra and is not considered here.

Brown et al. (1979) discussed the effective Hamiltonian [Eq. 3.19] for the $^2\Pi$ state in detail and calculated the corresponding matrix elements. Later Amiot et al. (1981) listed the matrix elements of the complete Hamiltonian for the $^2\Pi$ and $^2\Sigma^+$ states. The matrix elements of these Hamiltonians which are relevant to the present work are given in Table 3.1. The measured line positions are compared iteratively with the calculated line positions which are the appropriate differences between the term values of the upper and lower electronic states. These term values are obtained as the eigen values of the Hamiltonian matrix. In the computer

TABLE 3.1 Matrix elements of the Hamiltonian for states $^2\Sigma^+$ and $^2\Pi$

Molecular constant	Labelling[a]	Matrix element[b,c]
T_v	1,1	1
	2,2	1
	3,3	1
B_v	1,1	$x(x\mp1)$
	2,2	x^2-1
	3,3	x^2+1
	2,3	$-(x^2-1)^{1/2}$
D_v	1,1	$x^2(x\mp1)^2$
	2,2	$-x^2(x^2-1)$
	3,3	$-x^2(x^2+3)$
	2,3	$2x^2(x^2-1)^{1/2}$
γ_v	1,1	$0.5(x\mp1)$
A_v	2,2	0.5
	3,3	-0.5
A_{Dv}	2,2	$0.5(x^2-1)$
	3,3	$-0.5(x^2+1)$
p_v	3,3	$\mp0.5x$
q_v	3,3	$\mp x$
	2,3	$\pm0.5x(x^2-1)^{1/2}$

[a]Labels 1, 2, and 3 refer to states $^2\Sigma^+$, $^2\Pi_{3/2}$, and $^2\Pi_{1/2}$, respectively.

[b]$x = J + 0.5$.

[c]In the notation $\pm$ and $\mp$ the upper and lower signs refer to the e and f levels, respectively (see Brown et al., 1975).

program, the matrix formed with the matrix elements listed in Table 3.1 is diagonalized to obtain the eigen values, i.e., the term values of the upper and lower states involved in the transition. The molecular constants appear as adjustable parameters in the effective Hamiltonian. An improved set of molecular constants is generated from a least-squares fit of the calculated line positions to the observed ones. This non-linear least-squares procedure is repeated until a satisfactory set of molecular constants is obtained.

(ii) Method of merging

In the analysis of the molecular spectra, multiple estimates of a given molecular parameter are often obtained. These multiple estimates can be reduced to a single 'best possible' estimate in several ways. Among these, the method of 'merging' is often used in molecular spectroscopy. In this method, multiple estimates of the molecular constants obtained from the individual bands by the method of least-squares are combined together, taking into account their uncertainties and the correlations existing among them. In the present work the molecular constants were obtained by analyzing the rotational structure of the individual bands using the effective Hamiltonian proposed by Brown et al. (1979). These molecular constants, their standard deviations, and their variance-covariance matrices are used as input parameters for the correlated least-squares merging fit. The relation between these input parameters and the best "possible estimates"

obtained as output parameters in the merging procedure is given by the set of equations in matrix notation as (similar to Eq. 3.6)

$$Y = X\beta + \delta. \qquad [3.23]$$

Here Y, β, and δ are the column vectors representing the input parameters, the output parameters, and the unknown errors respectively; the coefficient matrix X relates the values of Y to the values of β. The least-squares solution of Eq. [3.23] gives molecular constants β as output parameters in such a way that the squares of the deviations are minimized subject to the inter-relations among δ. The equation for $\hat{\beta}$ (the symbol $\hat{}$ indicates that it is an estimate from the least-squares fit) in matrix notation is given by

$$\hat{\beta} = (X^T\Phi^{-1}X)^{-1}\, X^T\Phi^{-1}Y, \qquad [3.24]$$

where Φ is a nondiagonal generalized weight matrix, which is composed of the variance-covariance matrices obtained from the band by band fits. The estimated variance $\hat{\sigma}^2$ is given by

$$\hat{\sigma}^2 = (Y - X\beta)^T\, \Phi^{-1}(Y - X\beta)/f, \qquad [3.25]$$

where f is the number of degrees of freedom. The merged dispersion matrix is written as

$$\hat{V} = (X^T\Phi^{-1}X)^{-1}. \qquad [3.26]$$

The estimated variance-covariance matrix $\hat{\theta}$ which is associated with $\hat{\beta}$ is given by

$$\hat{\theta} = \hat{\sigma}^2\hat{V}. \qquad [3.27]$$

The uncertainties in the merged molecular constants which are obtained as output parameters are the square roots of the diagonal elements of the matrix $\hat{\theta}$. For further details of the

method of merging the reader is referred to Albritton et al. (1977), Coxon (1978), and Prasad and Reddy (1988).

3.3 The rotational structure of a band of a $^2\Pi_i$ - $^2\Sigma^+$ transition

A $^2\Pi_i$ state consists of a series of rotational levels for each of the substates $^2\Pi_{1/2}$ (J = 0.5, 1.5, ...) and $^2\Pi_{3/2}$ (J = 1.5, 2.5, ...) with the levels of $^2\Pi_{3/2}$ having lower energy than the corresponding levels of $^2\Pi_{1/2}$. The $^2\Pi$ state is called an inverted state because the spin-orbit coupling constant A is negative. It belongs to Hund's case (a) because A is large in magnitude. Normally a $^2\Sigma$ state belongs to Hund's case (b). The splitting of a $^2\Sigma$ state is due to the magnetic moment produced by the motion of the nuclei and precession of the electronic orbital angular momentum about the internuclear axis. As the two states $^2\Pi_i$ and $^2\Sigma^+$ belong to Hund's cases (a) and (b), respectively, a $^2\Pi_i$ - $^2\Sigma^+$ transition is known as a mixed case transition.

The rotational structure of a band arising from a $^2\Pi_i$ - $^2\Sigma^+$ transition consists of twelve branches. The selection rules to be satisfied in this transition are

$\Delta J = 0$ $\quad e \longleftrightarrow f$

$\Delta J = \pm 1$ $\quad e \longleftrightarrow e,\ f \longleftrightarrow f$

$+ \longleftrightarrow -,\ + \not\leftrightarrow +,\ - \not\leftrightarrow -.$

The twelve different branches are designated in accordance with the selection rules given above as R_{21ee}, R_{22ff}, Q_{21fe}, Q_{22ef},

P_{21ee}, P_{22ff}, R_{11ee}, R_{12ff}, Q_{11fe}, Q_{12ef}, P_{11ee}, and P_{12ff}. A schematic energy level diagram showing all the twelve branches is given in Fig. 7, in which the parity of the levels is indicated in the e/f notation given by Kopp and Hougen (1967) and Brown et al. (1975). If the bands of this system degrade to longer wavelengths, as in the case of comet-tail system, then the R_{12ee}, Q_{21fe}/R_{22ff}, R_{11ee}, and Q_{11fe}/R_{12ff} branches form four different heads in the rotational structure of the band. Each band of this system has two band origins, one for each of the $^2\Pi_{1/2} - {}^2\Sigma^+$ and $^2\Pi_{3/2} - {}^2\Sigma^+$ sub-bands. In the present work, instead of two origins, only the $(T_{v\Pi} - T_{v\Sigma})$ value is determined. The band origins of the two sub-systems can be calculated from $(T_{v\Pi} - T_{v\Sigma}) \pm (1/2)(A_v - 2B_v)$.

3.4 Rotational analysis of the comet-tail system of CO'

The spectrum of the cathode glow of the hollow-cathode discharge tube (described in Chapter 2), photographed in the region 3345 - 8500 Å under medium dispersion is shown in Fig. 8. In this figure, in addition to the 17 bands of the comet-tail system of CO^+, several bands belonging to the Baldet-Johnson ($B^2\Sigma^+ - A^2\Pi_i$) system of CO^+, the Ångström ($B^1\Sigma^+ - A^1\Pi$) and the Herzberg ($C^1\Sigma^+ - A^1\Pi$) systems of the neutral molecule CO are also identified. The vacuum wavenumbers of the band heads of the comet-tail system of CO^+, their relative intensities and vibrational quantum numbers are given in Table 3.2. The four heads identified for each band are formed by

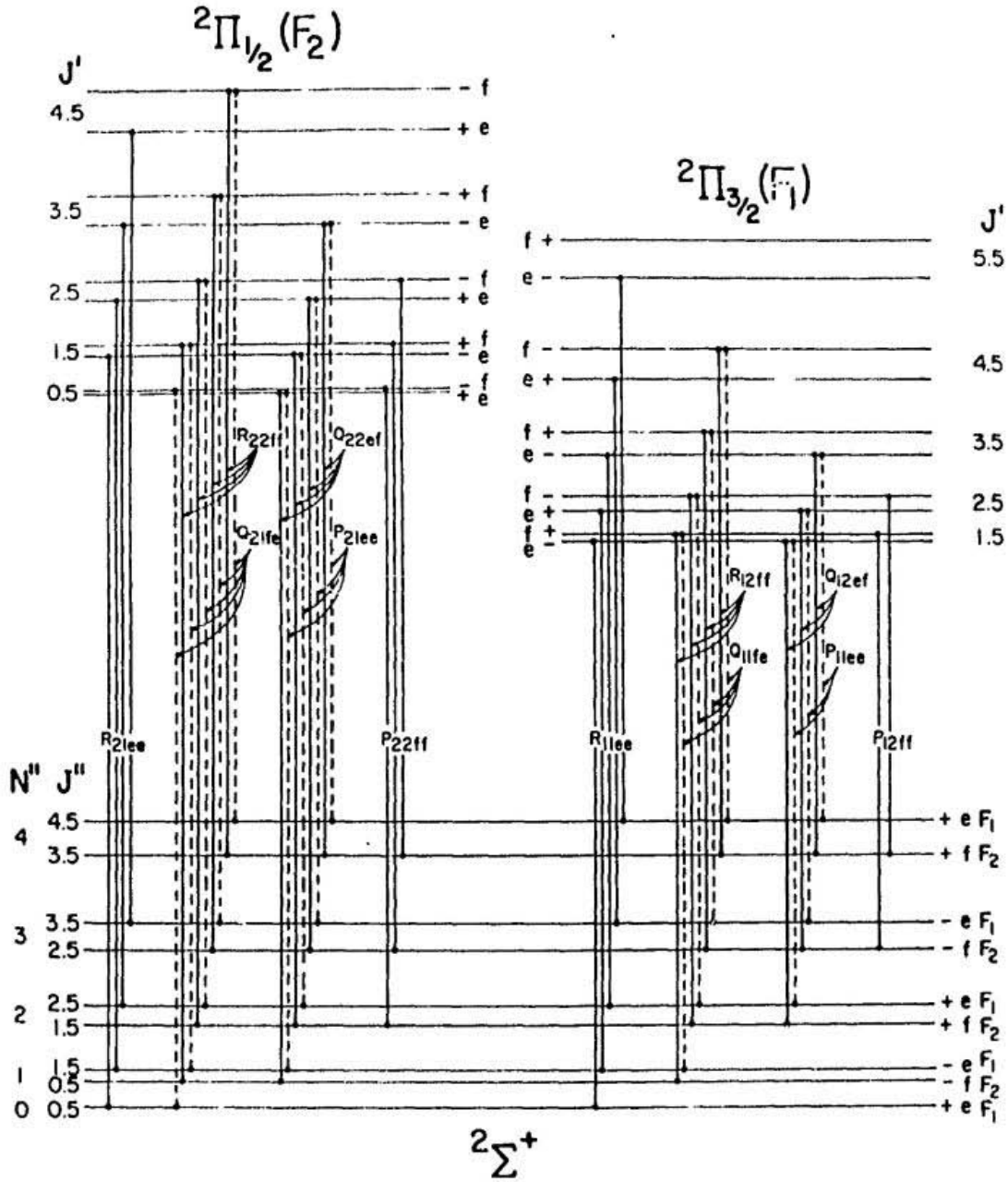

Figure 7. A schematic energy level diagram showing the first few rotational transitions of all the twelve branches of a band of a $^2\Pi_i - {}^2\Sigma^+$ transition.

Figure 8. The band systems produced in the cathode glow of the hollow-cathode discharge tube by exciting the CO gas in the region 3345-8500 Å. (a) Baldet-Johnson ($B^2\Sigma^+ - A^2\Pi_i$) system of CO^+; (b) comet-tail ($A^2\Pi_i - X^2\Sigma^+$) system of CO^+; (c) Ångström ($B^1\Sigma^+ - A^1\Pi$) system of CO; and (d) Herzberg ($C^1\Sigma^+ - A^1\Pi$) system of CO. This spectrum is photographed on the 2 m Bausch and Lomb spectrograph in the first order of a 600 grooves/mm grating.

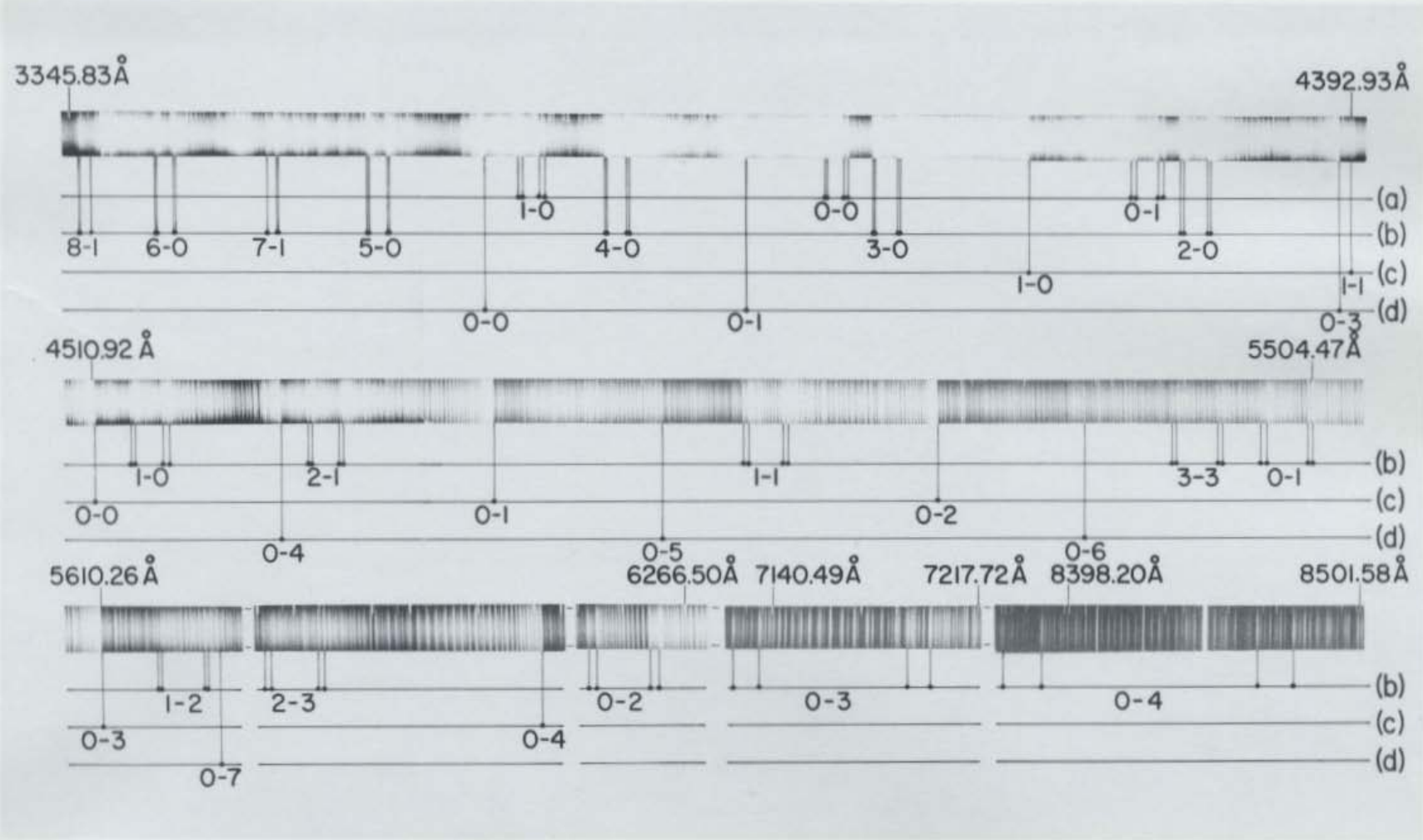
3345.83Å
4392.93Å
8-1
6-0
7-1
5-0
1-0
4-0
0-0
0-1
0-0
3-0
1-0
0-1
2-0
1-1
0-3
(a)
(b)
(c)
(d)
4510.92 Å
5504.47Å
1-0
2-1
1-1
3-3
0-1
0-0
0-1
0-2
0-4
0-5
0-6
5610.26 Å
6266.50Å
7140.49Å
7217.72Å
8398.20Å
8501.58Å
1-2
2-3
0-2
0-3
0-4
0-3
0-4
0-7

TABLE 3.2 Comet-tail ($A^2\Pi_i$ - $X^2\Sigma^+$) band system of the $^{12}C^{16}O^+$ molecule

Band head[a] (cm^{-1})	$T'_v - T''_v$[b] (cm^{-1})	Relative[c] intensity	Assignment v' - v"
29826.11[d] 29817.05[d] - 29692.28[d]		vw	8-1
29288.41 29276.55 29163.94 29153.11	29212.897(2)	w	6-0
28484.47[d] - 28367.51[d] 28347.42[d]		w	7-1
27891.72 27878.69 27763.28 27751.66		m	5-0
26462.56 26449.20 26336.38 26324.35	26384.760(2)	s	4-0
25009.13 24994.99 24882.58 24870.02	24930.349(2)	vs	3-0
23529.04 23514.03 23402.24 23388.97	23449.261(2)	vs	2-0
22022.07 22006.17 21895.08 21880.93	21941.217(1)	m	1-0
21345.58 21330.09 21218.80 21204.94	21265.232(1)	m	2-1
19839.22 19822.66 19712.03 19697.31	19757.570(2)	m	1-1

TABLE 3.2 (Continued)

Band head[a] (cm^{-1})	$T'_v - T''_v$[b] (cm^{-1})	Relative[c] intensity	Assignment v'- v"
18550.12[d]		vw	3-3
18535.64[d]			
18424.15[d]			
18409.14[d]			
18305.32	18222.329(2)	s	0-1
18287.64			
18177.66			
18162.05			
17685.77[d]		vw	1-2
17674.91[d]			
17559.40[d]			
17542.94[d]			
17070.47	16988.471(2)	vw	2-3
17053.51			
16943.22			
16928.20			
16152.50	16068.576(2)	s	0-2
16133.97			
16024.72			
16008.45			
14030.53	13945.479(2)	m	0-3
14011.01			
13902.43			
13885.44			
11938.78	11852.563(2)[e]	w	0-4
11918.26			
11810.34			
11792.68			

[a]The four heads identified for each band are formed by R_{21ee}, Q_{21fe}/R_{22ff}, R_{11ee}, and Q_{11fe}/R_{12ff} branches in the order of decreasing wavenumber.

[b]The number in the parentheses indicates the uncertainty in the last digit and corresponds to one standard deviation.

[c]The abbreviations for the relative intensities vs, s, m, w, and vw represent very strong, strong, medium, weak, and very weak respectively.

[d]Band head is measured under the medium dispersion.

[e]This value is obtained from the analysis of the 0-4 band and is not included in the merging.

R_{21ee}, Q_{21fe}/R_{22ff}, R_{11ee}, and Q_{11fe}/R_{12ff} in the order of decreasing wavenumber. The measurements of the band heads are made on high dispersion plates for 13 bands and on medium dispersion plates for the remaining 4 bands as indicated in Table 3.2.

Of the thirteen bands of the comet-tail system photographed under high resolution the rotational structure of twelve bands (6-0, 4-0, 3-0, 2-0, 1-0, 2-1, 1-1, 0-1, 2-3, 0-2, 0-3, and 0-4) was analyzed. Of these twelve bands, the rotational structure of six (6-0, 1-0, 2-1, 1-1, 0-1, and 0-2) was analyzed for the first time since Rao (1950a) decreased the vibrational assignment of the upper state by 3 units and identified the state as an inverted $^2\Pi$ state. The rotational structure of the 4-0 and 1-1 bands of this system photographed under high resolution on the 3.4 m Jarrell-Ash spectrograph are shown in Figs. 9 and 10, respectively. In these figures, the expected twelve branches in their rotational structures are clearly identified. The pairs of branches R_{22ff} and Q_{21fe}, Q_{22ef} and P_{21ee}, R_{12ff} and Q_{11fe}, and Q_{12ef} and P_{11ee} are due to the spin splitting of the rotational levels of the $X^2\Sigma^+$ state. As the value of the constant γ_v which represents the spin splitting of the rotational levels of the $X^2\Sigma^+$ state, is very small the actual splitting of the rotational lines could not be shown clearly for the 4-0 and 1-1 bands. The rotational quantum numbers and the vacuum wavenumbers of the spectral lines of all the twelve branches analyzed in the present work are listed in Table 3.3. The effective Hamiltonians of the $^2\Pi$

Figure 9.

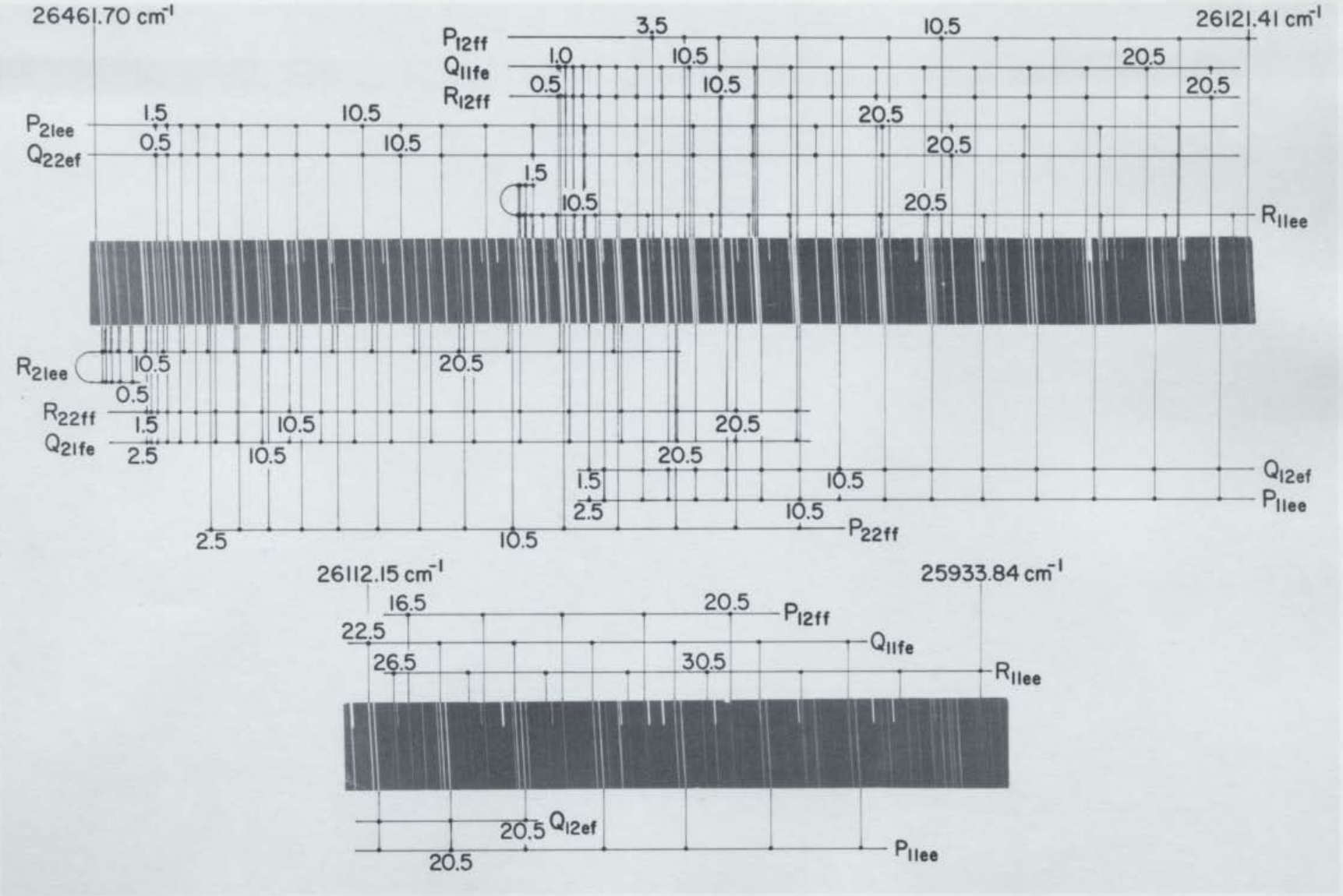
26461.70 cm⁻¹
26121.41 cm⁻¹
P12ff
Q11fe
R12ff
P21ee
Q22ef
R11ee
R21ee
R22ff
Q21fe
Q12ef
P11ee
P22ff
26112.15 cm⁻¹
25933.84 cm⁻¹
P12ff
Q11fe
R11ee
Q12ef
P11ee

Figure 10. Rotational structure of the 1-1 band of the comet-tail ($A^2\Pi_i - X^2\Sigma^+$) system of $^{12}C^{16}O^+$, photographed on the 3.4 m Jarrell-Ash spectrograph in the second order of a 1200 grooves/mm grating.

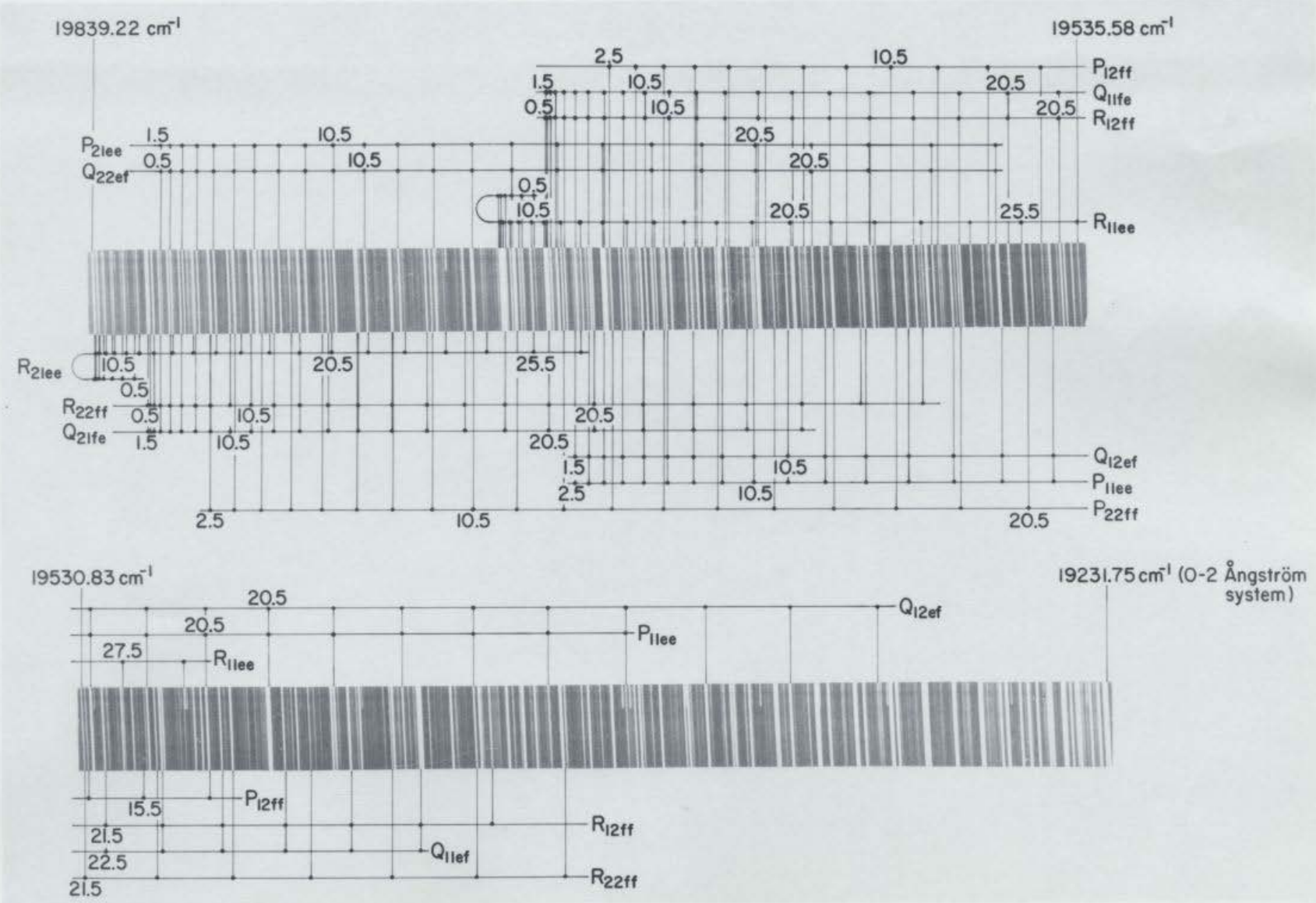
19839.22 cm⁻¹
19535.58 cm⁻¹
P21ee
Q22ef
R21ee
R22ff
Q21fe
P12ff
Q11fe
R12ff
R11ee
Q12ef
P11ee
P22ff
19530.83 cm⁻¹
19231.75 cm⁻¹ (0-2 Ångström system)
Q12ef
P11ee
R11ee
P12ff
R12ff
Q11ef
R22ff

TABLE 3.3 Vacuum wavenumbers (in cm^{-1}) of the rotational lines of the bands of the $A^2\Pi_i - X^2\Sigma^+$ system of $^{12}C^{16}O^+$

6-0 Band ($A^2\Pi_{1/2} - X^2\Sigma^+$)

J	$R_{21ee}(J)$	$R_{22ff}(J)$	$Q_{21fe}(J)$	$Q_{22ef}(J)$	$P_{21ee}(J)$	$P_{22ff}(J)$
0.5	29280.45(1)	29276.55(1)		29272.07(0)		
1.5	83.88(-2)	76.09(0)	29276.55(1)	68.65(1)	29272.07(0)	
2.5	86.39(1)	74.67(1)	76.09(0)	64.24(0)	68.65(1)	
3.5	87.90(0)	72.26(0)	74.67(1)	58.86(-1)	64.24(0)	
4.5	88.41(-2)	68.89(1)	72.26(0)	52.54(2)	58.86(-1)	29239.27(-1)
5.5	87.93(-6)	64.52(-1)	68.89(1)	45.18(-1)	52.54(-1)	29.03(1)
6.5	86.52(-5)	59.19(0)	64.52(-1)	36.90(0)	45.18(-1)	17.79(1)
7.5	84.16(-2)	52.88(-1)	59.19(0)	27.61(-2)	36.90(0)	05.64(6)
8.5	80.78(-1)	45.59(0)	52.88(-1)	17.36(-1)	27.61(-2)	29192.47[a]
9.5		37.34(3)	45.59(0)	06.15(1)	17.35(-1)	78.30[a]
10.5		28.11[a]	37.34(3)	29193.93(0)	06.15(1)	63.08(-2)
11.5		17.79(-1)	28.11[a]	80.74(1)	29193.93(2)	
12.5		06.54(-2)	17.79(-1)	66.56(1)	80.74(1)	
13.5		29194.32(1)	06.54(-2)	51.38(0)	66.56(1)	
14.5			29194.32(1)	35.26(5)	51.38(0)	
15.5				18.09(4)	35.26(5)	
16.5					18.09(4)	

TABLE 3.3 (Continued)

6-0 Band ($A^2\Pi_{3/2}$ - $X^2\Sigma^+$)

J	$R_{11ee}(J)$	$R_{12ff}(J)$	$Q_{11fe}(J)$	$Q_{12ef}(J)$	$P_{11ee}(J)$	$P_{12ff}(J)$
0.5	29157.02(-2)	29153.11(0)				
1.5	60.35(1)	52.48(2)	29153.11(0)	29145.24(0)		
2.5	62.56(-2)	50.77(-2)	52.48(2)	40.68(0)	29145.24(0)	
3.5	63.78(-1)	48.06(0)	50.77(-2)	35.05(-1)	40.68(0)	
4.5	63.94(0)	44.28(-1)	48.06(0)	28.38(-2)	35.05(-1)	29115.40(-1)
5.5	63.08(1)	39.48(0)	44.28(-1)	20.71(0)	28.38(-2)	04.83(1)
6.5	61.13(-1)	33.65(2)	39.48(0)	11.97(0)	20.71(0)	29092.94[a]
7.5	58.16(0)	26.75(2)	33.65(2)	02.17(-1)	11.97(0)	80.79[a]
8.5	54.12(-1)	18.79(2)	26.75(2)	29091.37(2)	02.17(-1)	66.58[a]
9.5	49.05(-1)	09.78(0)	18.79(2)	79.50(1)	29191.37(2)	51.97[a]
10.5	42.93(-1)	29099.75(1)	09.78(0)	66.58(1)	79.50(1)	36.26(-2)
11.5	35.76(0)	88.66(2)	29099.75(1)	52.61(1)	66.58(1)	19.42(-3)
12.5		76.47(-3)	88.64(-1)	37.58(-1)	52.61(1)	
13.5			76.47(-3)	21.53(0)	37.58(-1)	
14.5					21.53(0)	

TABLE 3.3 (Continued)

4-0 Band ($A^2\Pi_{1/2}$ - $X^2\Sigma^+$)

J	$R_{21ee}(J)$	$R_{22ff}(J)$	$Q_{21fe}(J)$	$Q_{22ef}(J)$	$P_{21ee}(J)$	$P_{22ff}(J)$
0.5	26453.24(-1)			26444.74(-2)		
1.5	56.85(-5)	26449.07(0)		41.46(1)	26444.74(-1)	
2.5	59.64(-2)	47.94(3)	26449.07(2)	37.25(0)	41.46(3)	26429.61(-6)
3.5	61.51(-1)	45.85(1)	47.94(5)	32.15(0)	37.25(2)	21.50(-4)
4.5	62.48(-1)	42.90(-1)	45.86(4)	26.13(-2)	32.15(3)	12.48(-5)
5.5	62.56(1)	39.07(1)	42.90(3)	19.28(1)	26.13(1)	02.62(1)
6.5	61.70(-2)	34.33(2)	39.04(2)	11.50(2)	19.23(1)	26391.75(-5)
7.5	60.00(1)	28.66(-1)	34.27(1)	02.78(-2)	11.42(-1)	80.07(-2)
8.5	57.37(1)	22.13(0)	28.62(0)	26393.21(-1)	02.72(-2)	67.49(0)
9.5	53.82(-2)	14.71(1)	22.08(1)	82.75(0)	26393.13(-3)	54.01(1)
10.5	49.40(0)	06.36(0)	14.62(-1)	71.40(2)	82.66(-2)	39.60(-2)
11.5	44.07(0)	26397.11(-1)	06.29(0)	59.13(2)	71.29(-1)	24.35(2)
12.5	37.86(2)	86.94(-4)	26397.06(2)	45.96(2)	59.00(-2)	08.15(0)
13.5	30.70(0)	75.93(-1)	86.91(2)	31.88(0)	45.83(-2)	26291.02(-5)
14.5	22.67(1)	63.95(-4)	75.84(0)	16.96(4)	31.75(-3)	73.05(-6)
15.5	13.70(0)	51.12(-3)	63.91(2)	01.08(2)	16.78(-3)	54.23(0)
16.5	03.83(-2)	37.41(1)	51.05(1)	26284.30(1)	00.91(-3)	
17.5	26393.09(0)	22.71(-2)	37.29(1)	66.62(0)	26284.14(-3)	
18.5	81.41(1)	07.16(-1)	22.64(3)	48.05(0)	66.51(1)	
19.5	68.83(0)	26290.63(-7)	07.04(0)	28.57(-1)	47.12(0)	
20.5	55.38(5)	73.22(-9)	26290.50(-6)	08.21(1)	28.45(1)	
21.5	40.95(3)	55.06(3)	73.22(5)	26186.93(0)	08.05(-1)	
22.5	25.58(-1)		54.81(7)	64.70(-5)	26186.78(0)	
23.5	09.35(-1)			41.60(-6)	64.58(0)	
24.5					41.50(1)	

TABLE 3.3 (Continued)

4-0 Band ($A^2\Pi_{3/2} - X^2\Sigma^+$)

J	$R_{11ee}(J)$	$R_{12ff}(J)$	$Q_{11fe}(J)$	$Q_{12ef}(J)$	$P_{11ee}(J)$	$P_{12ff}(J)$
0.5		26324.35(0)				
1.5	26331.75(0)	23.90(0)	26324.35(1)	26316.50(1)		
2.5	34.26(0)	22.47(-2)	23.90(2)	12.06(-5)	26316.50(2)	
3.5	35.81(0)	20.10(0)	22.47(1)	06.77(1)	12.06(-3)	26296.33(-5)
4.5	36.38(0)	16.76(1)	20.07(0)	00.45(-1)	06.74(1)	86.07(-3)
5.5	35.99(0)	12.44(1)	16.69(-2)	26293.17(1)	00.41(0)	76.86(1)
6.5	34.62(0)	07.16(2)	12.39(0)	84.96(5)	26293.12(0)	65.56(-8)
7.5	32.28(-1)	00.91(1)	07.08(-2)	75.69(0)	84.86(0)	53.41(-6)
8.5	29.00(1)	26293.70(2)	00.81(-2)	65.56(4)	75.65(1)	40.30(-2)
9.5	24.72(-1)	85.52(3)	26293.61(0)	54.38(0)	65.44(-1)	26.20(-2)
10.5	19.48(-2)	76.37(2)	85.41(-2)	42.29(2)	54.31(0)	11.14(-2)
11.5	13.28(-2)	66.26(2)	76.25(-2)	29.24(4)	42.19(-1)	26195.14(1)
12.5	06.13(-1)	55.19(2)	66.17(1)	15.21(4)	29.12(0)	78.15(1)
13.5	26297.98(-3)	43.13(0)	55.06(-2)	00.21(3)	15.10(2)	60.20(0)
14.5	88.90(-3)	30.17(4)	43.01(-2)	26184.27(4)	00.07(-1)	41.26(-3)
15.5	78.86(0)	16.20(3)	30.04(1)	67.32(1)	26184.11(-1)	21.41(-2)
16.5	67.84(-1)	01.23(-3)	16.07(1)	49.44(-1)	67.20(-1)	00.58(-3)
17.5	55.85(-2)	26185.38(0)	01.16(2)	30.64(2)	49.35(2)	26078.78(-5)
18.5	42.91(-2)	68.58(3)	85.24(-1)	10.81(-3)	30.50(0)	56.06(-3)
19.5	29.09(2)	50.69(-6)	68.42(1)	26090.07(-3)	10.74(3)	32.42(-1)
20.5	14.19(2)	31.92(-8)	50.60(-1)	68.36(-5)	26089.98(1)	07.78(-1)
21.5	26198.34(0)		31.87(1)		68.30(3)	
22.5	81.57(1)		12.15(1)		45.68*	
23.5	63.85(3)		26091.48(1)		21.95*	
24.5	45.11(0)		69.87(2)		25997.36*	
25.5	25.43(-2)		47.27(0)		71.75*	
26.5	04.83(-1)		23.74(1)			
27.5	26083.28(1)		25999.27(1)			
28.5	60.73(-2)		73.81(2)			
29.5	37.25(-2)					
30.5	12.84(1)					
31.5	25987.45(0)					
32.5	59.97*					
33.5	33.84(3)					
34.5	05.57(0)					

TABLE 3.3 (Continued)

3-0 Band ($A^2\Pi_{1/2}$ - $X^2\Sigma^+$)

J	$R_{21ee}(J)$	$R_{22ff}(J)$	$Q_{21fe}(J)$	$Q_{22ef}(J)$	$P_{21ee}(J)$	$P_{22ff}(J)$
0.5		24994.99(-1)		24990.37(-1)		
1.5	25002.69(-1)	94.83(0)	24994.99(0)	87.12(-1)	24990.37(1)	
2.5	05.58(0)	93.81(-1)	94.83(2)	82.99(-3)	87.12(1)	25975.34(0)
3.5	07.61(-1)	91.93(-2)	93.81(1)	78.04(-3)	82.99(0)	67.31(1)
4.5	08.81(1)	89.19(-2)	91.93(2)	72.22(-4)	78.04(1)	58.41(-1)
5.5	09.13(-1)	85.60(-2)	89.19(2)	65.55(-3)	72.22(0)	48.69(0)
6.5	08.58(-2)	81.15(-5)	85.60(3)	58.02(-3)	65.55(1)	38.09(0)
7.5	07.20(-2)	75.88(2)	81.15(3)	49.68(0)	58.02(2)	26.64(-1)
8.5	04.96(-1)	69.73(2)	75.79(-1)	40.44(0)	49.64(2)	14.34(0)
9.5	01.83(-2)	62.70(2)	69.66(2)	30.34(0)	40.38(1)	01.18(0)
10.5	24997.85(-3)	54.84(2)	62.59(-1)	19.39(1)	30.28(2)	24887.16(-1)
11.5	93.02(-2)	46.03(-3)	54.71(0)	07.57(0)	19.28(-2)	72.29(-1)
12.5	87.32(-2)	36.46(1)	45.95(-2)	24894.90(0)	07.45(-4)	56.57(-1)
13.5	80.76(-1)	25.99(1)	36.34(-1)	81.36(0)	23894.77(-3)	39.97(-2)
14.5	73.33(-1)	14.67(2)	25.86(-1)	66.99(2)	81.28(2)	22.54(-2)
15.5	65.01(-1)	02.47(2)	14.55(2)	51.73(2)	66.86(0)	04.23(-2)
16.5	55.85(0)	24889.39(0)	02.32(-1)	35.60(1)	51.61(2)	24785.15(3)
17.5		75.47(2)	24889.23(-2)		35.50(3)	65.12(3)
18.5		60.67(2)	75.32(0)			
19.5		44.98(1)	60.51(0)			
20.5		28.44(0)	44.79(-4)			
21.5		11.03(1)	28.24(-4)			
22.5		24792.86[a]	10.84(-2)			
23.5		73.55(-2)	24792.53[a]			
24.5			73.34(-6)			

TABLE 3.3 (Continued)

3-0 Band ($A^2\Pi_{3/2}$ - $X^2\Sigma^+$)

J	$R_{11ee}(J)$	$R_{12ff}(J)$	$Q_{11fe}(J)$	$Q_{12ef}(J)$	$P_{11ee}(J)$	$P_{12ff}(J)$
0.5	24873.95(0)	24870.02(0)				
1.5	77.51(-1)	69.65(-1)	24870.02(1)			
2.5	80.16(0)	68.37(-1)	69.65(1)	24857.87(0)		
3.5	81.89(1)	66.15(-2)	68.37(1)	52.64(-1)	24857.87(2)	
4.5	82.58(-8)	63.00(-3)	66.15(1)	46.48(-3)	52.64(2)	24832.99(0)
5.5	82.53(2)	58.93(-3)	63.00(1)	39.46(3)	46.48(1)	22.90(-2)
6.5	81.44(0)	53.93(-3)	58.93(2)	31.42(-1)	39.40(1)	11.90(-1)
7.5	79.42(-2)	48.05(2)	53.93(2)	22.49(-2)	31.37(-1)	24799.96(-2)
8.5	76.50(0)	41.20(3)	47.97(0)	12.63(-3)	22.44(-1)	87.14(1)
9.5	72.65(1)	33.41(2)	41.13(2)	01.85(-3)	12.57(-2)	73.34(0)
10.5	67.84(-1)	24.69(1)	33.29(-2)	24790.17(0)	01.79(-1)	58.64(0)
11.5	62.14(1)	15.07(3)	24.58(-2)	77.55(0)	24790.07(-2)	43.00(-1)
12.5	55.50(1)	04.47(-1)	14.94(-1)	63.99(1)	77.44(-1)	26.45(0)
13.5	47.90(-1)	24793.01(2)	04.35(-3)	49.52(1)	63.93(3)	09.00(2)
14.5	39.40(-1)	80.57(-1)	24792.86(-2)	34.11(0)	49.45(4)	24690.58(-1)
15.5	29.98(0)	67.26(2)	80.47(0)	17.79(-1)	37.05(5)	71.25(-2)
16.5	19.65(2)	52.99(1)	67.12(0)	00.52(-3)	17.64(-3)	51.00(-4)
17.5	08.35(0)	37.80(1)	52.85(0)	24682.33(-6)	00.46(3)	29.83(-5)
18.5	24796.17(1)	21.68(0)	37.66(0)	63.24(-7)	24682.25(-1)	27.81(0)
19.5	83.04(1)	04.65(-1)	21.57(3)	43.25(-6)	63.17(0)	24584.84(2)
20.5	64.99(1)	24686.67(-4)	04.53(0)	22.34(-7)	43.17(0)	60.96(4)
21.5	54.02(1)	67.81(-3)	24686.60(4)		23.23(-2)	36.09(-2)
22.5	38.13(2)		67.72(4)			10.40(2)
23.5	21.33(4)					24483.74(1)
24.5	03.55(0)					
25.5	24684.88(0)					
26.5	65.03(0)					
27.5	44.80(1)					
28.5	23.34(-3)					
29.5	01.04(2)					
30.5	24577.76(0)					

TABLE 3.3 (Continued)

2-0 Band ($A^2\Pi_{1/2}$ - $X^2\Sigma^+$)

J	$R_{21ee}(J)$	$R_{22ff}(J)$	$Q_{21fe}(J)$	$Q_{22ef}(J)$	$P_{21ee}(J)$	$P_{22ff}(J)$
0.5		23514.03(1)		23509.32(0)		
1.5	23521.79(1)	13.96(1)	23514.03(2)	06.12(-1)	23509.32(0)	23501.40(-7)
2.5	24.83(2)	13.06(0)	13.96(2)	02.11(-2)	06.12(0)	23494.35(-1)
3.5	27.04(0)	11.36(0)	13.09(4)	23497.29(-1)	02.11(0)	86.41(-1)
4.5	28.44(0)	08.85(0)	11.36(1)	91.63(-3)	23497.29(1)	77.68(0)
5.5	29.04(1)	05.50(-2)	08.15(2)	87.17(-4)	91.63(0)	68.19(8)
6.5	28.79(0)	01.34(-2)	05.50(1)	77.90(-4)	85.17(-1)	57.75(1)
7.5	27.74(1)	23496.37(-2)	01.34(1)	69.80(-4)	77.90(0)	46.55(0)
8.5	25.87(1)	90.57(-3)	23496.37(2)	60.90(-5)	69.80(0)	34.54(0)
9.5	23.17(0)	83.96(-3)	90.57(1)	51.16(-6)	60.90(-1)	21.72(1)
10.5	19.65(0)	76.53(-3)	83.96(2)	40.69(1)	51.16(-1)	08.08(0)
11.5	15.31(1)	68.29(-2)	76.53(2)	29.34(1)	40.60(-3)	23393.70(9)
12.5	10.14(-2)	59.20(6)	68.29(4)	17.15(0)	29.19(-9)	78.42(7)
13.5	04.16(-2)	49.38(4)	59.18(0)	04.15(-2)	17.04(-5)	62.34(8)
14.5	23497.33(-4)	38.67(5)	49.29(2)	23390.42(7)	04.06(-4)	45.42(6)
15.5	89.66(-8)	27.13(5)	38.54(-1)	75.78(5)	23390.32(3)	27.63(0)
16.5	81.21(-8)	14.74(3)	26.97(-4)	60.30(2)	75.67(1)	09.11(2)
17.5		01.50(-2)	14.59(-5)	44.00(-2)	60.22(2)	23289.73(0)
18.5		23387.55(4)	01.39(-5)	26.97(4)	43.94(0)	69.52(-4)
19.5		72.73(6)	23387.46(4)	09.11(9)	26.87(2)	48.50(-7)
20.5		57.05(5)	72.55(-3)		08.89(-4)	
21.5		40.50(0)	56.84(-6)			
22.5		23.14(-4)	40.29[a]			
23.5		04.92[a]	22.92[a]			
24.5		23286.02(-3)	04.71[a]			
25.5			23285.97(3)			

TABLE 3.3 (Continued)

2-0 Band ($A^2\Pi_{3/2}$ - $X^2\Sigma^+$)

J	$R_{11ee}(J)$	$R_{12ff}(J)$	$Q_{11fe}(J)$	$Q_{12ef}(J)$	$P_{11ee}(J)$	$P_{12ff}(J)$
0.5	23392.91(0)	23388.97(0)				
1.5	96.59(1)	88.72(0)	23388.97(0)	23381.10(-1)		
2.5	99.26(-8)	87.55(-1)	88.72(1)	76.91(-1)	23381.10(0)	
3.5	23401.15(-8)	85.46(-5)	87.55(0)	71.82(-1)	76.91(0)	
4.5	02.17(-3)	82.53(-4)	85.46(-3)	65.85(0)	71.82(1)	23352.17(0)
5.5	02.24(-6)	78.70(-4)	82.53(-1)	58.98(1)	65.85(2)	42.28(2)
6.5	01.50(1)	73.98(-3)	78.70(-1)	51.23(2)	58.98(4)	31.44(-1)
7.5	23399.78(-2)	68.34(-6)	73.98(0)	42.53(-2)	51.23(6)	19.77(0)
8.5	97.26(4)	61.87(-3)	68.34(-2)	32.97(-4)	42.53(1)	07.17(-2)
9.5	93.77(3)	54.57(7)	61.87(1)	22.54(-3)	32.97(0)	23293.73(1)
10.5	89.47(10)	46.28(6)	54.40(-6)	11.21(-5)	22.54(1)	79.38(1)
11.5		37.10(4)	48.18(1)	23299.12(7)	11.21(0)	64.12(-1)
12.5		27.05(5)	37.00(0)	86.02(7)	23299.01(2)	48.02(1)
13.5		16.05(-2)	26.87(-8)	72.05(8)	85.89(0)	30.98(-3)
14.5		04.27(3)	16.05(5)	57.19(8)	71.93(2)	13.12(-1)
15.5		23291.58(3)	04.20(2)	41.45(8)	57.06(1)	23194.34(-2)
16.5		77.98(2)	23291.46(-1)	24.80(6)	41.32(2)	74.70(-2)
17.5		63.45(-5)	77.87(-2)	07.29(5)	24.69(2)	54.12(-8)
18.5		48.07(-9)	63.40(-2)	23188.94(8)	07.15(-1)	32.75(-6)
19.5			47.98(-9)	69.66(6)	23188.75(-2)	
20.5				49.51(5)	69.47(-4)	
21.5				28.51(5)	49.27(-10)	
22.5				06.57(-1)	28.40(4)	
23.5				83.83(1)		

TABLE 3.3 (Continued)

1-0 Band ($A^2\Pi_{1/2}$ - $X^2\Sigma^+$)

J	$R_{21ee}(J)$	$R_{22ff}(J)$	$Q_{21fe}(J)$	$Q_{22ef}(J)$	$P_{21ee}(J)$	$P_{22ff}(J)$
0.5	22010.03(-1)	22006.13(0)		22001.39(-1)		
1.5	13.99(0)	06.17(0)	22006.13(1)	21998.25(-1)	22001.39(0)	21993.55(0)
2.5	17.16(0)	05.40(-3)	06.17(1)	94.33(-3)	21998.25(1)	86.49(0)
3.5	19.57(1)	03.88(-3)	05.40(0)	89.66(-2)	95.33(0)	70.07(0)
4.5	21.17(0)	01.58(-3)	03.88(0)	84.20(-2)	89.66(1)	60.69(0)
5.5	22.01(0)	21998.52(-3)	01.58(1)	77.96(-3)	84.20(2)	50.54(0)
6.5	22.07(-1)	94.67(-3)	21998.52(2)	70.94(-3)	77.96(2)	39.63(1)
7.5	21.36(0)	90.09(2)	94.67(2)	63.20(0)	70.94(2)	27.90(-1)
8.5	19.88(1)	84.68(0)	90.00(-2)	54.64(1)	63.12(-1)	15.43(-1)
9.5	17.60(0)	78.50(0)	84.62(0)	45.30(0)	54.56(0)	02.18(-2)
10.5	14.55(0)	71.55(0)	78.43(0)	35.19(0)	45.22(-1)	21888.12(-5)
11.5	10.74(2)	63.82(0)	71.48(0)	24.30(0)	35.09(-1)	73.34(-4)
12.5	06.11(-1)	55.30(-2)	63.74(0)	12.60(-3)	24.21(0)	
13.5			55.22(-1)		12.54(0)	

TABLE 3.3 (Continued)

1-0 Band ($A^2\Pi_{3/2} - X^2\Sigma^+$)

J	$R_{11ee}(J)$	$R_{12ff}(J)$	$Q_{11fe}(J)$	$Q_{12ef}(J)$	$P_{11ee}(J)$	$P_{12ff}(J)$
0.5	21884.85(0)	21880.93(0)				
1.5	85.62(1)	80.75(-1)	21880.93(1)	21873.06(-1)		
2.5	91.52(1)	79.72(-1)	80.75(1)	68.96(-2)	21873.06(0)	
3.5	93.54(-1)	77.85(-1)	79.72(1)	64.00(-2)	68.96(1)	21853.27(1)
4.5	94.76(1)	75.12(-1)	77.85(2)	58.19(-2)	64.00(1)	44.35(-2)
5.5	95.08(-1)	71.53(-2)	75.12(3)	51.52(-3)	58.19(1)	34.64(0)
6.5	94.57(0)	67.07(-4)	71.53(2)	44.03(-2)	51.52(1)	24.07(1)
7.5	93.20(-1)	61.82(0)	67.07(1)	35.70(1)	44.03(3)	12.58(-3)
8.5	91.00(0)	55.69(1)	61.77(0)	26.50(2)	35.62(-1)	00.33(0)
9.5	87.94(1)	48.69(-1)	55.62(0)	16.43(1)	26.40(-1)	21787.20(2)
10.5	84.01(-2)	40.86(0)	48.62(-1)	05.51(0)	16.33(-2)	73.21(1)
11.5	79.26(0)	32.20(1)	40.78(0)	21793.77(1)	05.43(0)	58.37(0)
12.5	73.67(0)	22.67(1)	32.10(0)	80.40[a]	21793.69(1)	42.68(-1)
13.5	67.23(1)	12.31(1)	22.56(-1)	67.71(-3)	80.40[a]	26.19(1)
14.5	59.92(-1)	01.09(-1)	12.18(-2)		67.66(2)	08.81(0)
15.5		21789.05(1)	00.97(-1)		53.35(-1)	21690.60(-2)
16.5			21788.94(1)			

TABLE 3.3 (Continued)

2-1 Band ($A^2\Pi_{1/2}$ - $X^2\Sigma^+$)

J	$R_{21ee}(J)$	$R_{22ff}(J)$	$Q_{21fe}(J)$	$Q_{22ef}(J)$	$P_{21ee}(J)$	$P_{22ff}(J)$
0.5	21333.90(-4)	21330.07(-1)		21325.38(-1)		
1.5	37.81(-2)	30.09(-1)	21330.07(0)	22.27(0)	21325.38(1)	
2.5	40.93(0)	29.34(0)	30.09(1)	18.37(-1)	22.27(2)	
3.5	43.27(0)	27.79(0)	29.34(3)	13.69(-2)	18.36(2)	21302.85(0)
4.5	44.81(-1)	25.49(1)	27.79(3)	08.25(-2)	13.69(2)	94.28(-2)
5.5	45.58(-1)	22.38(0)	25.49(4)	02.22(-4)	08.25(3)	84.94(-4)
6.5	45.58(0)	18.50(0)	25.38(5)	21295.04(1)	02.00(1)	74.85(-3)
7.5	44.79(-1)	13.82(-2)	18.45(1)	87.26(0)	21294.99(1)	63.96(-4)
8.5	43.21(0)	08.39(0)	13.77(0)	78.69(0)	87.18(-1)	52.30(-4)
9.5	40.85(-1)	02.17(1)	08.30(-1)	69.35(1)	78.61(-1)	39.86(-4)
10.5	37.70(-1)	21295.15(1)	02.06(-2)	59.22(0)	69.27(1)	26.82(-6)
11.5	33.79(2)	87.34(1)	21295.04(-1)	48.31(1)	59.11(-1)	12.65(-2)
12.5	29.08(4)	78.75(1)	87.23(-1)	36.60(1)	48.19(-1)	21197.85(-3)
13.5	23.58(6)	69.35(0)	78.63(0)	24.10(-1)	36.48(-1)	82.30(0)
14.5	17.27(7)	59.20(4)	69.22(-1)	10.84(1)	23.97(-2)	65.96(2)
15.5	10.07(0)	48.17(-1)	59.04(0)		10.73(3)	48.79(1)
16.5	02.15(0)					

TABLE 3.3 (Continued)

2-1 Band ($A^2\Pi_{3/2}$ - $X^2\Sigma^+$)

J	$R_{11ee}(J)$	$R_{12ff}(J)$	$Q_{11fe}(J)$	$Q_{12ef}(J)$	$P_{11ee}(J)$	$P_{12ff}(J)$
0.5	21208.83(0)	21204.94(0)				
1.5	12.53(0)	04.75(-1)	21204.94(1)	21197.16(0)		
2.5	15.38(-1)	03.72(-1)	04.75(1)	93.07(-1)	21197.16(2)	
3.5	17.37(-1)	01.82(-2)	03.72(2)	88.14(-1)	93.07(1)	21177.52(1)
4.5	18.52(-1)	21199.09(-1)	01.82(2)	82.36(-2)	88.14(2)	68.68(-1)
5.5	18.80(-1)	95.48(-3)	21199.09(3)	75.72(-3)	82.36(3)	59.03(0)
6.5	18.26(1)	91.04(-2)	95.48(3)	68.24(-2)	75.72(2)	48.50(0)
7.5	16.82(-1)	85.79(2)	91.04(4)	59.92(0)	68.24(2)	37.12(-1)
8.5	14.55(-1)	79.60(-1)	85.70(0)	50.73(0)	59.85(-1)	24.86(-4)
9.5	11.43(0)	72.61(1)	79.53(-1)	40.69(0)	50.67(1)	11.80(-3)
10.5	07.45(1)	64.76(1)	72.51(0)	29.79(0)	40.59(-1)	21097.89(0)
11.5	02.61(0)	56.03(0)	64.64(0)	18.04(0)	29.69(-1)	83.12(0)
12.5	21196.91(0)	46.46(0)	55.92(1)	05.43(0)	17.93(-1)	67.48(0)
13.5	90.40(5)	36.05(1)	46.31(-1)	21091.98(1)	05.93(1)	50.97(-3)
14.5		24.75(0)	35.93(4)	77.65(-1)	21091.85(-1)	
15.5		12.61(0)		62.49(-1)	77.55(1)	

TABLE 3.3 (Continued)

1-1 Band ($A^2\Pi_{1/2}$ - $X^2\Sigma^+$)

J	$R_{21ee}(J)$	$R_{22ff}(J)$	$Q_{21fe}(J)$	$Q_{22ef}(J)$	$P_{21ee}(J)$	$P_{22ff}(J)$
0.5	19826.40(0)	19822.52(-3)		19817.80(1)		
1.5	30.40(0)	22.66(0)	19822.52(-2)	14.71(-3)	19817.80(2)	
2.5	33.62(-2)	22.01(-2)	22.66(2)	10.92(-3)	14.71(-1)	19803.10(0)
3.5	36.16(0)	20.63(-5)	22.01(0)	06.39(-4)	10.92(-1)	19795.42(0)
4.5	37.95(3)	18.59(2)	20.63(-2)	01.13(-3)	06.39(-1)	87.02(0)
5.5	38.96(0)	15.73(-1)	18.59(5)	19795.15(-1)	01.13(1)	77.88(1)
6.5	39.22(-3)	12.15(0)	15.73(4)	88.43(1)	19795.10(-1)	68.01(1)
7.5	38.77(-3)	07.86(2)	12.15(5)	80.93(-1)	88.36(-1)	57.37(0)
8.5	37.62(2)	02.77(0)	07.76(-1)	72.72(1)	80.88(0)	48.00(-2)
9.5	35.68(0)	19796.97(0)	02.70(0)	63.76(0)	72.65(0)	33.91(-1)
10.5	32.99(0)	90.41(-1)	19796.93(4)	54.07(1)	63.67(-1)	21.08(-1)
11.5	29.59(1)	83.13(0)	90.37(3)	43.59(-2)	53.98(1)	07.51(0)
12.5	25.40(0)	75.11(1)	83.04(0)	32.45(2)	43.52(0)	19693.17(-3)
13.5	20.48(0)	66.31(1)	75.00(0)	20.48(-1)	32.34(1)	78.12(-2)
14.5	14.79(-2)	56.78(1)	66.21(1)	07.86(4)	20.40(0)	62.33(-1)
15.5	08.41(1)	48.48(-1)	56.65(-1)	19694.35(-5)	07.69(-2)	45.76(-3)
16.5	01.21(-1)	35.45(-1)	46.37(-1)	80.25(2)	19694.26(-3)	28.45(-5)
17.5	19793.28(-2)	23.68(0)	35.36(2)	65.31(0)	80.09(-1)	10.44(-3)
18.5	84.62(0)	11.16(2)	23.57(2)	49.65(1)	65.20(2)	19591.67(-2)
19.5	75.17(-1)	19697.86(1)	10.98(-2)	33.24(1)	49.52(1)	72.11(-4)
20.5	64.99(0)	83.83(0)	19697.71(1)	16.09(3)	33.09(1)	51.89(2)
21.5	54.03(-1)	69.00(1)	83.66(1)	19598.16(3)	15.93(3)	30.83(-1)
22.5	42.32(0)	53.44(1)	68.82(-2)	79.43(-2)	19597.94(-3)	09.06(0)
23.5	29.83(1)	37.13(2)	53.24(-2)	60.05(4)	79 28(0)	19486.53(1)
24.5	16.61(1)	19.99(-2)	36.96(3)		59.82(-2)	63.23(-1)
25.5	02.60(0)	02.16(0)	19.82(-1)			39.18(-1)
26.5	19687.83(1)	83.54(-1)				14.38(-1)
27.5		64.16(0)				19388.84(2)

TABLE 3.3 (Continued)

1-1 Band ($A^2\Pi_{3/2}$ - $X^2\Sigma^+$)

J	$R_{11ee}(J)$	$R_{12ff}(J)$	$Q_{11fe}(J)$	$Q_{12ef}(J)$	$P_{11ee}(J)$	$P_{12ff}(J)$
0.5	19701.18(0)	19697.31(1)				
1.5	04.97(-1)	97.21(1)	19697.31(2)	19689.53(2)		
2.5	07.86(-10)	96.26(-4)	97.21(2)	85.51(-2)	19689.53(4)	19677.86(2)
3.5	10.14(1)	94.54(-5)	96.26(-2)	80.72(-2)	85.51(0)	69.95(-2)
4.5	11.47(-1)	92.04(-2)	94.54(-2)	75.15(1)	80.72(1)	61.27(-1)
5.5	12.03(1)	88.67(-4)	92.04(2)	68.73(2)	75.15(5)	51.82(3)
6.5	11.72(-2)	84.53(-2)	88.67(1)	61.46(-1)	68.73(6)	41.47(0)
7.5	10.63(-2)	79.53(-5)	84.53(3)	53.44(2)	61.46(4)	30.34(-1)
8.5	08.72(-3)	73.78(-1)	79.53(1)	44.57(0)	53.40(3)	18.43(2)
9.5	06.04(2)	67.21(2)	73.78(6)	34.90(1)	44.48(-2)	05.68(2)
10.5	02.48(-1)	59.79(1)	67.12(0)	24.38(-2)	34.82(0)	19592.11(0)
11.5	19698.13(-1)	51.55(-1)	59.70(0)	13.13(2)	24.34(2)	77.75(2)
12.5	92.96(-2)	42.54(2)	51.43(-4)	00.98(-2)	13.04(2)	62.52(-4)
13.5	86.02(0)	32.68(0)	42.43(1)	19588.08(0)	00.89(-2)	46.58(1)
14.5	80.25(2)	28.01(-1)	32.57(0)	74.35(0)	19588.00(2)	29.77(0)
15.5	72.63(0)	10.57(2)	21.87(-3)	59.82(1)	74.27(3)	12.15(-1)
16.5	64.25(2)	19598.27(-1)	10.44(1)	44.45(-2)	59.70(0)	19493.68(-8)
17.5	54.99(-2)	85.18(-2)	19598.16(2)	28.29(-2)	44.36(2)	
18.5	44.99(2)	71.29(0)	86.06(2)	11.35(0)	28.16(-2)	
19.5	34.13(0)	56.58(-1)	71.12(-2)	19493.56(-2)	11.21(-1)	
20.5	22.50(2)	41.08(0)	56.44(1)	74.95(-6)	19493.45(1)	
21.5	10.02(-1)	24.74(-3)	40.89(-2)	55.65(3)	74.85(0)	
22.5	19596.76(0)	07.63(-1)	24.57(-1)	35.37(-6)	55.43(-3)	
23.5	82.64(-3)	19489.71(0)	07.42(-2)	14.43(-1)	35.27(0)	
24.5	67.79(1)	70.98(1)	19489.51(1)	19392.59(-5)	14.28(1)	
25.5	52.06(-2)	51.43(1)	70.76(1)	69.97(-6)	19392.47(1)	
26.5	35.58(1)	31.05(-2)	51.19(0)	48.65(2)	69.84(-1)	
27.5	18.25(0)	09.90(0)	30.80(-2)	22.45(3)		
28.5	00.09(-4)			19297.43(3)		

TABLE 3.3 (Continued)

0-1 Band ($A^2\Pi_{1/2}$ - $X^2\Sigma^+$)

J	$R_{21ee}(J)$	$R_{22ff}(J)$	$Q_{21fe}(J)$	$Q_{22ef}(J)$	$P_{21ee}(J)$	$P_{22ff}(J)$
0.5	18290.17[a]					
1.5	95.14[a]	18287.64(0)		18279.59[a]		
2.5	98.99[a]	87.17(2)	18287.64(0)	75.77[a]	18279.59[a]	18267.99(3)
3.5	18301.65[a]	85.96(-1)	87.17(2)	71.70[a]	75.77[a]	60.39(0)
4.5	03.66[a]	84.07(-1)	85.96(-1)	66.52[a]	71.70[a]	52.09(-3)
5.5	04.56[a]	81.53(3)	84.07(-1)	60.79[a]	66.52[a]	43.18(3)
6.5	05.32(-3)	78.23(2)	81.53(3)	53.96[a]	60.79[a]	33.50(2)
7.5	05.22(-2)	74.20(-1)	78.23(2)	46.92(-5)	53.96[a]	23.14(3)
8.5	04.42(-1)	69.51(-2)	74.20(-1)	39.10(2)	46.92(-5)	12.03(-2)
9.5	02.89(-2)	64.13(-1)	69.51(-2)	30.49(0)	39.10(2)	00.27(-2)
10.5	00.69(0)	58.02(-2)	64.13(-1)	21.18(-2)	30.49(0)	18187.85(4)
11.5	18297.79(3)	51.21(-3)	58.02(-2)	11.20(0)	21.18(-2)	74.64(-1)
12.5	94.16(3)	43.74(1)	51.21(-3)	00.46(-5)	11.20(0)	60.78(0)
13.5	89.77(-2)	35.51(-1)	43.74(1)	18189.12(2)	00.46(-5)	46.23(2)
14.5	84.72(-1)	26.59(0)	35.51(-1)	77.00(0)	18189.12(2)	30.91(-2)
15.5	78.97(0)	16.96(0)	26.59(0)	64.18(1)	77.00(0)	14.96(1)
16.5	72.49(0)	06.62(1)	16.96(0)	50.63(-2)	64.18(1)	18098.28(1)
17.5	65.31(1)	18195.60(5)	06.62(1)	36.43(2)	50.63(-2)	80.86(-1)
18.5	57.36(-3)	83.79(1)	18195.60(5)	21.46(1)	36.43(2)	62.75(-2)
19.5	48.74(-2)	71.32(4)	83.79(1)	05.81(1)	21.46(-1)	43.99(3)
20.5		58.06(-1)	71.32(4)	18089.46(3)	05.81(1)	
21.5		44.16(2)	58.06(-1)	72.35(2)	18089.46(3)	
22.5		29.49(0)	44.16(2)		72.35(2)	
23.5		14.12(-1)	29.49(0)			
24.5			14.12(-1)			

TABLE 3.3 (Continued)

O-1 Band ($A^2\Pi_{3/2}$ - $X^2\Sigma^+$)

J	$R_{11ee}(J)$	$R_{12ff}(J)$	$Q_{11fe}(J)$	$Q_{12ef}(J)$	$P_{11ee}(J)$	$P_{12ff}(J)$
0.5	18165.95(-1)	18162.05(-2)				
1.5	69.83(-2)	62.05(-2)	18162.05(-2)	18154.28(0)		
2.5	72.93(-4)	61.33(3)	62.65(-2)	50.43(4)	18154.28(0)	
3.5	75.33(3)	59.76(2)	61.33(3)	45.71(-1)	50.43(4)	
4.5	76.90(3)	57.40(-1)	59.76(2)	40.28(1)	45.71(-1)	
5.5	77.66(1)	54.28(-1)	57.40(-1)	34.06(1)	40.28(1)	
6.5	77.66(1)	50.43(3)	54.28(-1)	27.09(4)	34.06(1)	18106.77(-3)
7.5	76.90(2)	45.71(-3)	50.43(3)	19.28(1)	27.09(4)	18095.90(-2)
8.5	75.33(1)	40.28(-2)	45.71(-3)	10.79(8)	19.28(1)	84.25(0)
9.5	73.03(4)	34.06(-2)	40.28(-2)	01.32(-7)	10.79(8)	71.81(1)
10.5	69.91(2)	27.09(0)	34.06(-2)	18091.31(3)	01.32(-7)	58.10[a]
11.5	66.02(2)	19.35(2)	27.09(0)	80.39(-1)	18091.31(3)	44.60(0)
12.5	61.33(-2)	10.79(1)	19.35(2)	68.74(0)	80.39(-1)	29.86(3)
13.5	55.93(2)	01.46(0)	10.79(1)	56.35(3)	68.74(0)	14.33(4)
14.5	49.72(2)	18091.37(0)	01.46(0)	43.14(2)	56.35(3)	17998.02(4)
15.5	42.69(-3)	80.50(-1)	18091.37(0)	29.11(-4)	43.14(2)	
16.5	34.97[a]	68.89(2)	80.50(-1)	14.38(-1)	29.11(-3)	
17.5	26.41(-2)	56.44(-2)	68.89(2)	17998.85(-3)	14.38(-1)	
18.5		43.32[a]	56.44(-2)		17998.85(-3)	
19.5		29.36(3)	43.32[a]			
20.5		14.68[a]	29.36(3)			
21.5		17999.03(-8)	14.68[a]			
22.5		82.73[a]	17999.03(-8)			
23.5		65.79(-2)	82.73[a]			
24.5		47.99(0)	65.79(-2)			
25.5		29.43(1)	47.99(0)			
26.5			29.43(1)			

TABLE 3.3 (Continued)

2-3 Band ($A^2\Pi_{1/2}$ - $X^2\Sigma^+$)

J	$R_{21ee}(J)$	$R_{22ff}(J)$	$Q_{21fe}(J)$	$Q_{22ef}(J)$	$P_{21ee}(J)$	$P_{22ff}(J)$
0.5		17053.36(0)		17048.67(0)		
1.5	17061.13(0)	53.51(-1)	17053.36(0)	45.70(0)	17048.67(0)	17041.09(5)
2.5	64.42(3)	52.99(0)	53.51(0)	42.05(1)	45.70(0)	34.30(3)
3.5	66.98(3)	51.75(0)	52.99(0)	37.68(1)	42.05(1)	26.79(-1)
4.5	68.84(2)	49.83(2)	51.75(0)	32.61(1)	37.68(1)	18.65(2)
5.5	70.03(4)	47.15(-2)	49.83(2)	26.84(0)	32.61(1)	09.77(1)
6.5	70.47(2)	43.80(-2)	47.15(-2)	20.35(-2)	26.84(0)	00.14(-5)
7.5	70.18(-2)	39.76(-1)	43.80(-2)	13.19(-1)	20.35(-2)	16989.91(-2)
8.5	69.21(-3)	35.01(-1)	39.76(-1)	05.36(3)	13.19(-1)	78.92(-3)
9.5	67.57(-2)	29.51(-4)	35.01(-1)	16996.74(-1)	05.36(-3)	67.32(4)
10.5	65.20(-2)	23.35(-4)	29.51(-4)	87.45(-2)	16996.74(-1)	54.89(-1)
11.5	62.14(0)	16.53(2)	23.35(-4)	77.51(3)	87.45(-2)	41.84(2)
12.5	58.35(0)	08.92(0)	16.53(2)	66.79(0)	77.51(3)	28.02(-1)
13.5	53.86(1)	00.62(-1)	08.92(0)	55.39(1)	66.79(0)	13.52(-1)
14.5	48.63(0)	16991.58(-3)	00.62(-1)	43.28(1)	55.39(1)	16898.37(3)
15.5	42.69(-1)	81.92(3)	16991.58(-3)	30.45(0)	43.28(1)	82.43(0)
16.5	36.06(0)	71.44(0)	81.92(3)	16.93(3)	30.45(0)	65.82(1)
17.5	28.66(-2)	60.31(3)	71.44(0)	02.68(3)	16.93(3)	48.50(2)
18.5		48.37(-3)	60.31 (3)		02.68(3)	
19.5		35.80(0)	48.37(-3)			
20.5			35.80(0)			

TABLE 3.3 (Continued)

2-3 Band ($A^2\Pi_{3/2}$ - $X^2\Sigma^+$)

J	$R_{11ee}(J)$	$R_{12ff}(J)$	$Q_{11fe}(J)$	$Q_{12ef}(J)$	$P_{11ee}(J)$	$P_{12ff}(J)$
0.5	16932.04(-3)					
1.5	35.87(1)	16928.20(-3)				
2.5	38.86(0)	27.42(0)	16928.20(-3)	16916.77(0)		16909.15(-2)
3.5	41.08(-2)	25.84(1)	27.42(0)	12.16(1)	16916.77(0)	01.42[a]
4.5	42.54(-1)	23.47(0)	25.84(1)	06.74(0)	12.16(1)	16893.04(-2)
5.5	43.22(0)	20.33(1)	23.47(0)	00.57(0)	06.74(0)	83.83(-1)
6.5	43.14(2)	16.41(0)	20.33(1)	16983.63(2)	00.57(0)	73.85(0)
7.5	42.23(-1)	11.72(1)	16.41(0)	85.86(-2)	16893.63(2)	63.08(-1)
8.5	40.60(1)	06.25(0)	11.72(1)	77.37(0)	85.86(-2)	51.61[a]
9.5	38.13(-2)	16900.00(0)	06.25(0)	68.07(-2)	77.37(0)	39.36[a]
10.5	34.93(-1)	16892.97(-1)	16900.00(0)	58.05(2)	68.07(-2)	26.15(2)
11.5	30.96(1)	85.19(1)	16892.97(-1)	47.20(0)	58.05(2)	12.27(1)
12.5	26.23(3)	76.62(1)	85.19(1)	35.63(3)	47.20(0)	16797.65(3)
13.5	20.68(3)	67.26(-1)	76.62(1)	23.24(2)	35.63(3)	82.20(-1)
14.5	14.35(2)	57.15(1)	67.26(0)	10.05(-2)	23.24(2)	
15.5	07.28(4)	46.24(-1)	57.15(1)	16796.12(-2)	10.05(-2)	
16.5	16899.38(1)		46.24(0)	81.41(-3)	16796.12(-2)	
17.5				65.95(-2)	81.41(-3)	
18.5					65.95(-2)	

TABLE 3.3 (Continued)

0-2 Band ($A^2\Pi_{1/2}$ - $X^2\Sigma^+$)

J	$R_{21ee}(J)$	$R_{22ff}(J)$	$Q_{21fe}(J)$	$Q_{22ef}(J)$	$P_{21ee}(J)$	$P_{22ff}(J)$
0.5	16136.83*	16133.69(-1)				
1.5	41.53*	33.97(-2)	16133.69(0)	16125.89*		
2.5	45.17*	33.60(-2)	33.97(0)	22.18*	16125.89*	16114.43(0)
3.5	48.13*	32.59(0)	33.60(1)	18.39*	22.18*	06.87*
4.5	50.84*	30.91(0)	32.59(3)	13.04*	18.39*	16098.92(-1)
5.5	51.38*	28.55(-2)	30.91(4)	07.92*	13.04*	90.19(0)
6.5	52.34(-2)	25.56(1)	28.55(3)	01.29*	07.92*	80.82(2)
7.5	52.50(-1)	21.88(0)	25.51(2)	16094.54(-1)	01.29*	70.76(1)
8.5	52.03(2)	17.56(2)	21.81(-1)	87.06(0)	16094.54(1)	59.99(-4)
9.5	50.84(1)	12.53(0)	17.47(0)	78.86(0)	86.98(0)	48.60(-6)
10.5	49.00(0)	06.87(1)	12.49(0)	70.00(1)	78.79(1)	36.61(-2)
11.5	46.48(-1)	00.53(0)	06.79(1)	60.47(0)	69.92(1)	23.87(-6)
12.5	43.34(2)	16093.52(0)	00.41(-2)	50.27(-1)	60.40(2)	10.64(7)
13.5	39.49(1)	85.84(-1)	16093.39(-4)	39.43(0)	50.21(3)	15996.47(-8)
14.5	34.96(1)	77.49(-2)	85.70(-4)	27.91(0)	39.35(3)	81.78(-8)
15.5	29.76(-1)	68.48(1)	77.34(-5)	15.72(-1)	27.83(3)	66.47(-4)
16.5	23.90(0)	58.81(2)	68.32(-4)	02.81*	15.65(4)	
17.5	17.42(5)	48.42(-1)	58.62(-4)	15989.34(-1)	02.81*	
18.5	10.14(-1)	37.40(2)	48.25(-4)	75.15(-1)	15989.16(-5)	
19.5	02.26(1)	25.66(0)	37.20(-3)		75.06(5)	
20.5	16093.67(0)	13.26(1)	25.50(2)			
21.5	84.41(-1)	00.24(6)	13.09(-1)			
22.5	74.47(-1)		00.01(0)			
23.5	63.86(1)					

TABLE 3.3 (Continued)

0-2 Band ($A^2\Pi_{3/2}$ - $X^2\Sigma^+$)

J	$R_{11ee}(J)$	$R_{12ff}(J)$	$Q_{11fe}(J)$	$Q_{12ef}(J)$	$P_{11ee}(J)$	$P_{12ff}(J)$
0.5						
1.5		16008.45(-1)		16000.65(-2)		
2.5	16019.35(0)	07.74(-1)	16008.45(1)	15996.88(-2)	16000.65(1)	
3.5	21.82(1)	06.40(-1)	07.79(1)	92.37(-2)	15996.88(1)	
4.5	23.53(1)	04.25(-3)	06.40(2)	87.12(-2)	92.37(2)	
5.5	24.51(1)	01.42(0)	04.25(1)	81.13(-2)	87.12(2)	15963.99(-2)
6.5	24.72(-1)	15997.78(-2)	01.42(5)	74.39(-3)	81.13(2)	56.23*
7.5	24.23(1)	93.45(1)	15997.78(3)	66.95(-1)	74.39(2)	43.57(-3)
8.5	22.98(0)	88.38(0)	93.40(0)	58.77(1)	66.89(-1)	32.25(-4)
9.5	21.00(0)	82.53(-3)	88.28(1)	49.83(1)	58.70(1)	20.20(-5)
10.5	18.27(0)	75.96(-5)	82.45(0)	40.16(1)	49.76(1)	07.53(6)
11.5	14.84(3)	68.65(-8)	75.89(0)	29.76(1)	40.07(0)	15893.98(2)
12.5	10.64(2)	60.71(0)	68.59(1)	18.57(-3)	29.63(-2)	79.67(5)
13.5	05.73(4)	51.84(-11)	60.53(-1)	06.70(-3)	18.53(2)	
14.5	00.01(0)		51.77(0)	15894.11(-1)	06.58(-5)	
15.5	15993.63(3)			80.76(-1)	15894.01(0)	
16.5	86.48(2)			66.70(-1)	80.60(-5)	
17.5				51.92(2)	66.53(-4)	
18.5				36.36(-1)	51.75(-1)	
19.5				20.10(0)	36.19(-3)	
20.5				03.11(1)	19.93(-2)	
21.5				15785.39(1)	02.93(-1)	
22.5				66.97(4)	15785.22(1)	
23.5				47.80(5)	66.74(-2)	
24.5					47.58(1)	

TABLE 3.3 (Continued)

0-3 Band ($A^2\Pi_{1/2}$ - $X^2\Sigma^+$)

J	$R_{21ee}(J)$	$R_{22ff}(J)$	$Q_{21fe}(J)$	$Q_{22ef}(J)$	$P_{21ee}(J)$	$P_{22ff}(J)$
0.5	14015.85*	14010.65(3)				
1.5	19.86*	11.01(4)	14010.65(3)	14002.98*		
2.5	22.18*	10.70(0)	11.01(4)	13999.31*	14992.98*	13991.54(0)
3.5	25.22*	14009.83(1)	10.70(0)	95.62*	13999.31*	84.26(-1)
4.5	27.00*	08.33(2)	09.83(1)	90.83*	95.62*	76.37(0)
5.5	28.87*	06.19(2)	08.33(2)	85.55*	90.83*	67.88(1)
6.5	30.10(-2)	03.43(1)	06.19(2)	79.29*	85.55*	58.75(2)
7.5	30.53(-2)	00.05(1)	03.43(1)	72.85(-7)	79.29*	49.01(4)
8.5	30.33(-3)	13996.05(1)	00.05(1)	65.69(-3)	72.85(-7)	38.63(4)
9.5	29.50(-4)	91.42(1)	13996.05(1)	57.86(-4)	65.69(-3)	27.63(4)
10.5	28.09(-1)	86.15(0)	91.42(1)	49.44(-2)	57.86(-4)	16.00(4)
11.5	26.00(-1)	80.29(2)	86.15(0)	40.39(0)	49.44(-2)	03.73(2)
12.5	23.30(-1)	73.77(2)	80.29(2)	30.68(-2)	40.39(0)	13890.85(1)
13.5	19.97(-1)	66.61(0)	73.77(2)	20.38(0)	30.68(-2)	77.36(2)
14.5	15.96(-5)	58.86(3)	66.61(0)	09.40(-4)	20.38(0)	63.24(3)
15.5	11.37(-4)	50.46(3)	58.86(3)	13897.85(-1)	09.40(-4)	48.47(1)
16.5		41.40(1)	50.46(3)	85.61(-4)	13897.85(-1)	33.11(4)
17.5		31.74(3)	41.40(1)	72.77(-3)	85.61(-4)	17.08(3)
18.5		21.41(2)	31.74(3)	59.31(-1)	72.77(-3)	00.50(9)
19.5		10.48(3)	21.41(2)	45.20(0)	59.31(-1)	13783.21(8)
20.5		13898.91(5)	10.48(3)	30.42(-3)	45.20(0)	65.31 (9)
21.5			13898.91(5)	15.05(-3)	30.42(-4)	
22.5				13799.03(-2)	15.04(-3)	
23.5				82.37(-2)	13799.03(-2)	
24.5				65.09(0)	82.37(-2)	
25.5				47.13(0)	65.09(0)	
26.5					47.13(0)	

TABLE 3.3 (Continued)

0-3 Band ($A^2\Pi_{3/2}$ - $X^2\Sigma^+$)

J	$R_{11ee}(J)$	$R_{12ff}(J)$	$Q_{11fe}(J)$	$Q_{12ef}(J)$	$P_{11ee}(J)$	$P_{12ff}(J)$
0.5	13889.14(2)	13885.31(1)				
1.5	93.09(1)	85.44(-1)	13885.31(1)			
2.5	96.36(1)	84.89(-2)	85.44(-1)	13874.00(-1)		
3.5	98.91(0)	83.66(1)	84.89(-2)	69.65(0)	13874.00(-1)	
4.5	13900.75(-3)	81.72(1)	83.66(1)	64.59(0)	69.65(0)	
5.5	01.94(-1)	79.03(-3)	81.72(1)	58.83(1)	64.59(0)	
6.5	02.43(2)	75.71(0)	79.03(-3)	52.35(-1)	58.83(1)	13832.11(-1)
7.5	02.18(1)	71.67(1)	75.71(0)	45.20(0)	52.35(-1)	21.85(0)
8.5	01.24(0)	66.90(-1)	71.67(1)	37.34(0)	45.20(0)	10.88(0)
9.5	13899.60(0)	61.47(0)	66.90(-1)	28.77(-1)	37.34(0)	13799.06*
10.5	97.26(0)	55.32(0)	61.47(0)	19.52(0)	28.77(-1)	86.83(0)
11.5	94.24(0)	48.47(-1)	55.32(0)	09.57(0)	19.52(0)	73.76(-1)
12.5	90.49(0)	40.94(0)	48.47(-1)	13798.92(0)	09.57(0)	59.99(-1)
13.5	86.07(0)	32.69(0)	40.94(0)	87.57(0)	13798.92(1)	45.53(-2)
14.5	80.95(1)	23.75(-1)	32.69(0)	75.52(-1)	87.57(0)	30.39(0)
15.5	75.12(0)	14.14(1)	23.75(-1)	62.77(-1)	75.52(-1)	14.57(3)
16.5	68.60(0)	03.80(-1)	14.14(1)	49.35(0)	62.77(-1)	13698.01(1)
17.5	61.36(-2)	13792.80(1)	03.80(-1)	35.21(-1)	49.35(0)	
18.5	53.48(0)	81.08(0)	13792.80(1)	20.39(-1)	35.21(-1)	
19.5	44.86(0)	68.71(4)	81.08(0)	04.88(-1)	20.39(-1)	
20.5	35.54(-2)		68.71(4)	13688.70(1)	04.88(-1)	
21.5	25.55(-2)			71.80(1)	13688.70(1)	
22.5	14.90(2)			54.23(3)	71.80(1)	
23.5	03.49(0)				54.23(3)	
24.5	13791.45(3)					
25.5	78.66(1)					
26.5	65.16(-3)					
27.5	51.06(2)					

TABLE 3.3 (Continued)

0-4 Band ($A^2\Pi_{1/2}$ - $X^2\Sigma^+$)

J	$R_{21ee}(J)$	$R_{22ff}(J)$	$Q_{21fe}(J)$	$Q_{22ef}(J)$	$P_{21ee}(J)$	$P_{22ff}(J)$
0.5	11920.84[a]	11917.83(0)				
1.5	25.24[a]	18.26(0)	11917.83(1)	11910.15[a]		
2.5	30.39[a]	18.10(-2)	18.26(1)	07.13[a]	11910.1 [a]	
3.5	32.61[a]	17.38(-1)	18.10(-1)	03.11[a]	07.13[a]	
4.5	34.85(0)	16.05(-3)	17.38(1)	11898.53[a]	03.11[a]	11884.12(1)
5.5	36.54[a]	14.18(-1)	16.05(0)	93.50[a]	11898.53[a]	75.85(1)
6.5	37.98(0)	11.70(-1)	14.18(2)	87.67[a]	93.50[a]	66.92(-4)
7.5	38.66(-1)	08.63(-1)	11.70(3)	81.30(-5)	87.67[a]	57.53(1)
8.5	38.78(1)	04.93(-4)	08.63(3)	74.44(-5)	81.30(-1)	47.48(-1)
9.5	38.28(0)	00.72(-1)	04.93(0)	66.92[a]	74.44(0)	38.84[a]
10.5	37.21(1)	11895.90(0)	00.72(4)	59.01(-1)	66.92[a]	25.69(1)
11.5	35.54(0)	90.49(1)	11895.85(0)	50.41(0)	58.98(1)	13.89(0)
12.5	33.27(-1)	84.49(2)	90.40(-2)	41.20(-1)	50.36(1)	01.52(0)
13.5	30.45(1)	77.86(-2)	84.42(1)	31.42(-1)	41.14(-1)	11788.56(-1)
14.5	26.99(-2)	70.68(1)	77.79(-1)	21.05(-1)	31.36(-1)	75.02(0)
15.5	22.97(-1)	62.91(2)	70.64(4)	10.10(0)	20.99(0)	60.89(-1)
16.5		54.50(-1)	62.80(-1)	11798.58(2)	10.05(3)	46.20(1)
17.5		45.54(0)	54.42(-1)	86.44(1)	11798.48(1)	30.86(-2)
18.5		-	45.46(1)	73.70(0)	86.33(-1)	14.96(-4)
19.5		25.80(-2)	-	60.37(-2)	73.61(-1)	
20.5		15.06(0)	25.69(-4)	46.51(1)	60.29(0)	
21.5		03.64(-7)	14.96(0)		46.39(0)	
22.5		11791.75(-2)	03.61(1)			
23.5			11791.66(0)			

TABLE 3.3 (Continued)

0-4 Band ($A^2\Pi_{3/2}$ - $X^2\Sigma^+$)

J	$R_{11ee}(J)$	$R_{12ff}(J)$	$Q_{11fe}(J)$	$Q_{12ef}(J)$	$P_{11ee}(J)$	$P_{12ff}(J)$
0.5	11796.21(-1)	11792.30[a]				
1.5	11800.24(1)	92.68(0)	11792.30[a]	11783.93[a]		
2.5	03.57(0)	92.23(-2)	92.68(1)	81.33(-1)	11783.93[a]	
3.5	06.27(2)	91.15(-1)	92.23(0)	77.14(0)	81.33(1)	
4.5	08.28(1)	89.38(-2)	91.15(1)	72.27(0)	77.14(2)	
5.5	09.63(0)	86.96(-3)	89.38(0)	66.72(-1)	72.27(3)	
6.5	10.32(1)	83.87(-4)	86.96(0)	60.53(-1)	66.72(2)	
7.5	10.34(0)	80.16(-2)	83.87(0)	53.65(-3)	60.53(3)	11730.30(-2)
8.5	09.72(1)	75.74(-4)	80.16(2)	46.15(-1)	53.65(1)	19.70(0)
9.5	08.41(-1)	70.72(0)	75.74(0)	38.00(0)	46.15(3)	08.40(-1)
10.5	06.45(0)	65.00(0)	70.63(-1)	29.15(0)	37.96(2)	11696.47(0)
11.5	03.83(-1)	58.63(-1)	64.90(-1)	19.66(0)	29.09(-1)	83.88(1)
12.5	00.54(-2)	51.60(0)	58.53(1)	09.51(0)	19.61(1)	70.63(1)
13.5	11796.63(0)	43.89(-3)	51.49(1)	11698.71(0)	09.44(0)	56.71(-1)
14.5	92.08(5)	35.58(-1)	43.79(1)	87.24(-1)	11698.63(-1)	
15.5	86.83(4)	26.52(-8)	35.44(2)	75.13(0)	87.16(-2)	
16.5	80.90(1)		26.44(2)	62.40(3)	75.06(-2)	
17.5	74.36(3)			48.98(1)	62.30(0)	
18.5	67.12(0)			34.89(0)	48.86(-1)	
19.5	59.26(1)				34.78(-3)	
20.5	50.75(1)					
21.5	41.55(-2)					
22.5	31.78(3)					
23.5	21.27(-2)					

[a]Not included in the analysis.

and $^2\Sigma^+$ states whose matrix elements are given in Table 3.1 were used in analyzing the rotational structure of the bands. The vacuum wavenumbers of the spectral lines of all the branches of a given band were simultaneously used as input in the non-linear least-squares program. The molecular constants and their standard deviations were obtained from the least-squares fit. In general, the standard deviation of the least-squares fit is found to be ~ 0.03 cm^{-1}.

The molecular constants obtained from the analysis of eleven bands (6-0, 4-0, 3-0, 2-0, 1-0, 2-1, 1-1, 0-1, 2-3, 0-2, and 0-3) were merged together. Nine molecular constants (B_v, D_v, and γ_v for the $X^2\Sigma^+$ state and B_v, D_v, A_v, A_{Dv}, p_v, and q_v for the $A^2\Pi_i$ state) and the band origin ($T'_v - T''_v$) were estimated from the analysis of the individual bands. The spin splitting constant γ_v of $X^2\Sigma^+$ and the Λ-doubling parameters p_v and q_v of $A^2\Pi_i$ could not be estimated for some weak bands. These molecular constants, their standard deviations, and the corresponding variance-covariance matrices were used as input data for the Merge 1. As the 0-4 band is weak and diffuse a good set of molecular constants could not be estimated from its wavenumber data and hence the resulting constants were not included in the merging. In the Merge 1, the 101 initial parameters obtained from the analysis of the individual bands were reduced to 58 parameters (12 band origins, 6 each of B_v, D_v, A_v, A_{Dv}, p_v, and q_v for v = 0 to 4 and v = 6 for $A^2\Pi_i$, 4 each of B_v and D_v for v = 0 to 3, and γ_0, γ_1, and γ_2 for $X^2\Sigma^+$). The

$T'_v - T''_v$ values thus obtained are listed in Table 3.2 and the rotational constants are listed in Table 3.4. These band origins and the rotational constants, their standard deviations, and the corresponding dispersion matrix are used as input for the next merge (discussed in Chapter 4) in which all the experimental data on CO' were merged together.

TABLE 3.4 Rotational constants[a] (in cm^{-1}) of the $A^2\Pi_i$ and $X^2\Sigma^+$ states of $^{12}C^{16}O^+$

$A^2\Pi_i$						
v	B_v	$D_v \times 10^6$	$-A_v$	$-A_{Dv} \times 10^4$	$p_v \times 10^2$	$q_v \times 10^4$
0	1.57784(3)	5.75(4)	122.053(2)	4.72(9)	1.28(2)	-1.12(25)
1	1.55877(3)	5.67(4)	122.000(2)	2.38(7)	1.07(2)	0.43(13)
2	1.53912(3)	6.68(6)	121.894(2)	5.17(13)	1.14(2)	-1.90(33)
3	1.52014(3)	7.44(5)	121.823(3)	3.22(16)	0.44(3)	3.80(27)
4	1.50061(3)	7.00(5)	121.861(3)	4.30(13)	0.90(3)	-0.23(24)
5	1.482469[b]					
6	1.46293(7)	13.88(3)	120.385(3)	5.76(33)	1.63(6)	-1.3(1.1)

$X^2\Sigma^+$			
v	B_v	$D_v \times 10^6$	$\gamma_v \times 10^3$
0	1.96623(3)	7.09(6)	6.06(10)
1	1.94674(3)	4.71(4)	8.0(1)
2	1.92741(4)	4.96(6)	7.3(2)
3	1.90833(3)	5.01(5)	

[a]The number in the parentheses indicates the uncertainty in the last digit and correspond to one standard deviation.

[b]Calculated from the expression $B_v = B_e - \alpha_e(v + 1/2)$.

CHAPTER 4

GLOBAL FIT OF THE EXPERIMENTAL DATA OF CO^+

The present study on the CO^+ molecule is aimed at obtaining a precise set of molecular constants for the three well established electronic states $X^2\Sigma^+$, $A^2\Pi_i$, and $B^2\Sigma^+$ by a method of global merging. In addition to the comet-tail ($A^2\Pi_i$ - $X^2\Sigma^+$) system of CO^+, discussed in Chapter 3, the first negative ($B^2\Sigma^+$ - $X^2\Sigma^+$) system (Rao, 1950b and Misra *et al.*, 1987), the Baldet-Johnson ($B^2\Sigma^+$ - $A^2\Pi_i$) system (Jakubek *et al.*, 1987), and the microwave data of the v = 0, 1, and 2 levels of $X^2\Sigma^+$ (Sastry *et al.*, 1981 and Bogey *et al.*, 1983) were reanalysed using the effective Hamiltonians of $^2\Pi$ (Brown *et al.*, 1979) and $^2\Sigma^+$ states. All the molecular constants and the band origins obtained from these analyses were combined by the method of correlated least-squares fit and all the multiple estimates were reduced to a single set of values. The details of this correlated least-squares fit are given in Section 3.2(ii). The vibrational term values of all the observed levels and the vibrational constants ω_e, $\omega_e x_e$, and $\omega_e y_e$ of the three electronic states were estimated from the band-origin data. The rotational constants obtained from the global fit were used in estimating the equilibrium rotational constants B_e and α_e. The moment of inertia I_e and the equilibrium internuclear distance r_e were calculated for the three electronic states using the corresponding B_e values.

4.1 The first negative ($B^2\Sigma^+ - X^2\Sigma^+$) system

The rotational structure of a $^2\Sigma - ^2\Sigma$ transition, in which both the electronic states belong to Hund's case (b), consists of two series of doublets, one series corresponding to $\Delta N = +1$ (R branch) and the other to $\Delta N = -1$ (P branch). The P series consists of the P_{11ee} and P_{22ff} branches, and a satellite branch $^{P}Q_{12ef}$, and the R series consists of the R_{11ee} and R_{22ff} branches, and a satellite branch $^{R}Q_{21fe}$. The two satellite branches $^{P}Q_{12ef}$ and $^{R}Q_{21fe}$ are normally very weak and in most cases may not even be observed. A schematic energy level diagram showing all the six branches is given in Fig. 11. Here the subscripts 1 and 2 refer to the F_1 and F_2 components, respectively, and e and f refer to the parities of the rotational levels. If the spin splitting of the spectral lines is not fully resolved, only one R and one P branch would be observed, instead of two for each branch. If the bands are degraded to longer wavelengths as in the case of the B-X system, R branch forms the head.

In the present work, the experimental data of the 12 bands (0-3, 0-4, 1-2, 1-3, 1-4, 1-5, 2-3, 2-4, 2-5, 2-6, 3-5, and 4-7) reported by Rao (1950b) and the 3 bands (0-0, 0-1, and 0-2) reported by Misra et al. (1987) were reanalysed and the molecular constants were estimated using the effective Hamiltonian of a $^2\Sigma^+$ state. The details of the method of analysis and the matrix elements of the $^2\Sigma^+$ state used in the Hamiltonian are given in Chapter 3. The values of the molecular constants and their standard deviations along with

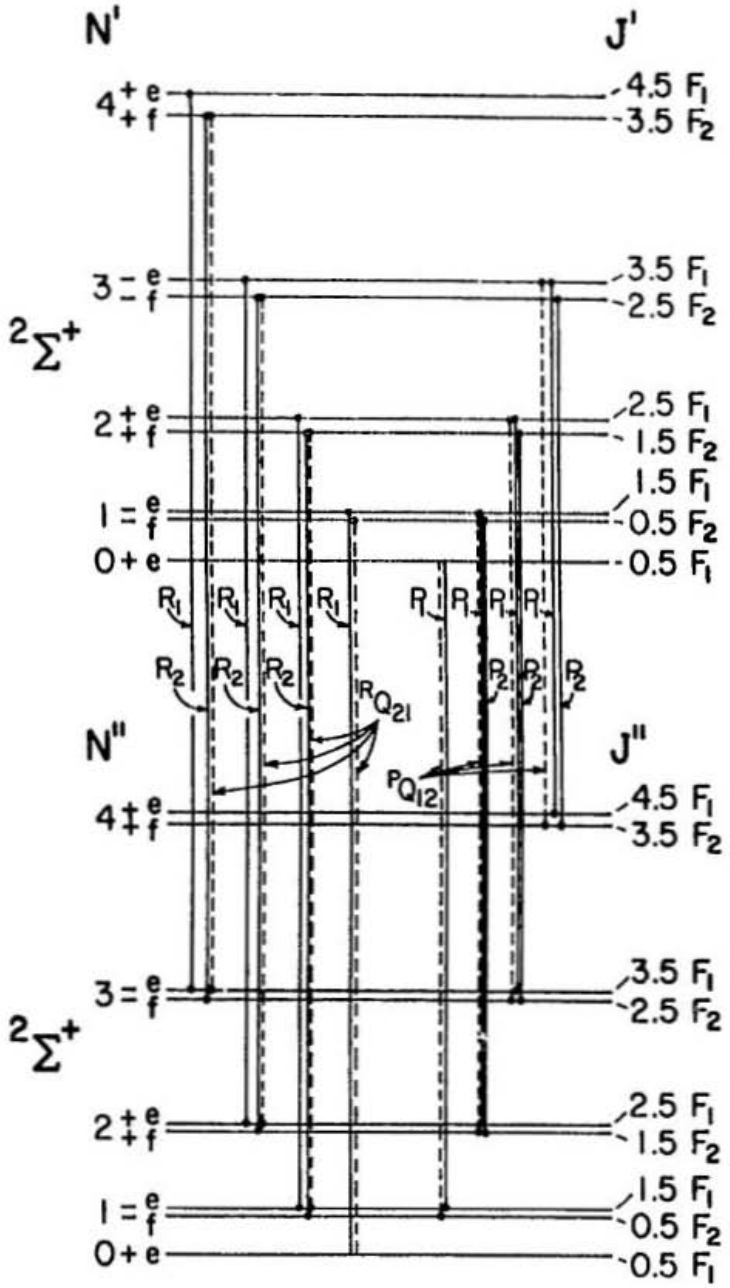

Figure 11. A schematic energy level diagram showing the first few rotational transitions of all the six branches of a band of a $^2\Sigma^+ - {}^2\Sigma^+$ transition.

the variance-covariance matrices obtained from the band by band analysis were used as the input data for Merge 2 (Merge 1 is discussed in Section 3.4). In this merge 89 initial parameters were reduced to 49 parameters (13 band origins, 5 for each of B'_v, D'_v, and γ'_v, and 7 for each of B''_v, D''_v, and γ''_v). The 36 rotational constants (B_v, D_v, and γ_v) obtained from Merge 2 are given in Table 4.1. The molecular constants thus obtained agree well with the values reported by Misra et al. (1987). The controversy over the $|\gamma'_v - \gamma''_v|$ differences of the bands of this system existing in the literature is reexamined. Although the γ_v values reported in the present work for various vibrational levels of states X and B are slightly different from those of Misra et al. (1987), the $|\gamma'_v - \gamma''_v|$ values are in good agreement with those reported by them and Rao (1950b). The $|\gamma'_v - \gamma''_v|$ values presented in Table IV in the Appendix show that the values reported by Woods (1943) are relatively very high.

4.2 The Baldet-Johnson ($B^2\Sigma^+ - A^2\Pi_i$) system

The Baldet-Johnson system arises from a transition between a $^2\Sigma^+$ [Hund's case (b)] state and $^2\Pi_i$ [Hund's case (a)] state, thus representing a mixed case transition. The rotational structure of a band arising from a $^2\Sigma^+ - ^2\Pi_i$ transition consists of twelve different branches. The selection rules to be satisfied in this transition are

TABLE 4.1 Rotational constants[a] (in cm^{-1}) of the $B^2\Sigma^+$ and $X^2\Sigma^+$ states of CO^+ obtained from the B-X system

v	B_v	$D_v \times 10^6$	γ_v
	$B^2\Sigma^+$		
0	1.78462(2)	8.029(8)	0.025(1)
1	1.75445(3)	8.214(13)	0.025(1)
2	1.72411(2)	8.422(11)	0.027(1)
3	1.69363(6)	8.507(29)	0.024(1)
4	1.66409(12)	8.98(97)	0.009(4)
	$X^2\Sigma^+$		
0	1.96723(2)	6.288(9)	0.016(1)
2	1.92924(3)	6.362(14)	0.016(1)
3	1.91011(2)	6.392(9)	0.016(1)
4	1.89093(2)	6.431(10)	0.018(1)
5	1.87156(3)	6.394(14)	0.017(1)
6	1.85234(3)	6.535(14)	0.020(1)
7	1.83332(12)	6.71(10)	0.006(4)

[a]Number in the parentheses is the uncertainty in the last digit and corresponds to one standard deviation.

$\Delta J = 0$ $\quad e \leftrightarrow f$

$\Delta J = \pm 1$ $\quad e \leftrightarrow e,\ f \leftrightarrow f$

$+ \leftrightarrow -,\ + \not\leftrightarrow +,\ - \not\leftrightarrow -.$

The twelve different branches in this system are identified as, P_{12ee}, P_{22ff}, Q_{12ef}, Q_{22fe}, R_{12ee}, R_{22ff}, P_{11ee}, P_{21ff}, Q_{11ef}, Q_{21fe}, R_{11ee}, and R_{21ff}. Here the subscripts 1 and 2 refer to the F_1 and F_2 components, respectively, and e and f refer to the parities of the rotational levels. A schematic energy level diagram showing all 12 branches of a band of a $^2\Sigma^+ - {}^2\Pi_i$ transition in Fig. 12. If the bands of a system are degraded to shorter wavelengths as in the case of the Baldet-Johnson system, the P_{12ee} and P_{22ff}/Q_{12ef} branches form two heads of the $^2\Sigma^+ - {}^2\Pi_{1/2}$ subband and the P_{11ee} and P_{21ff}/Q_{11ef} branches form two heads of the $^2\Sigma^+ - {}^2\Pi_{3/2}$ subband.

In the present work, the experimental data of the 3 bands (1-0, 0-0, and 0-1) reported by Jakubek et al. (1987) were reanalysed and the molecular constants were estimated using the effective Hamiltonians of the $^2\Pi_i$ and $^2\Sigma^+$ states. The details of the method of analysis along with the matrix elements for the Hamiltonians of the $^2\Pi$ and $^2\Sigma^+$ states are given in Chapter 3. The values of the molecular constants, their standard deviations and the variance co-variance matrices obtained from the band by band analysis were used as the input data for Merge 3. In this merge, 33 initial parameters were reduced to 23 parameters (3 band origins, 3 for each of B_v, D_v, and γ_v for v = 0 and 1 levels of the $B^2\Sigma^+$

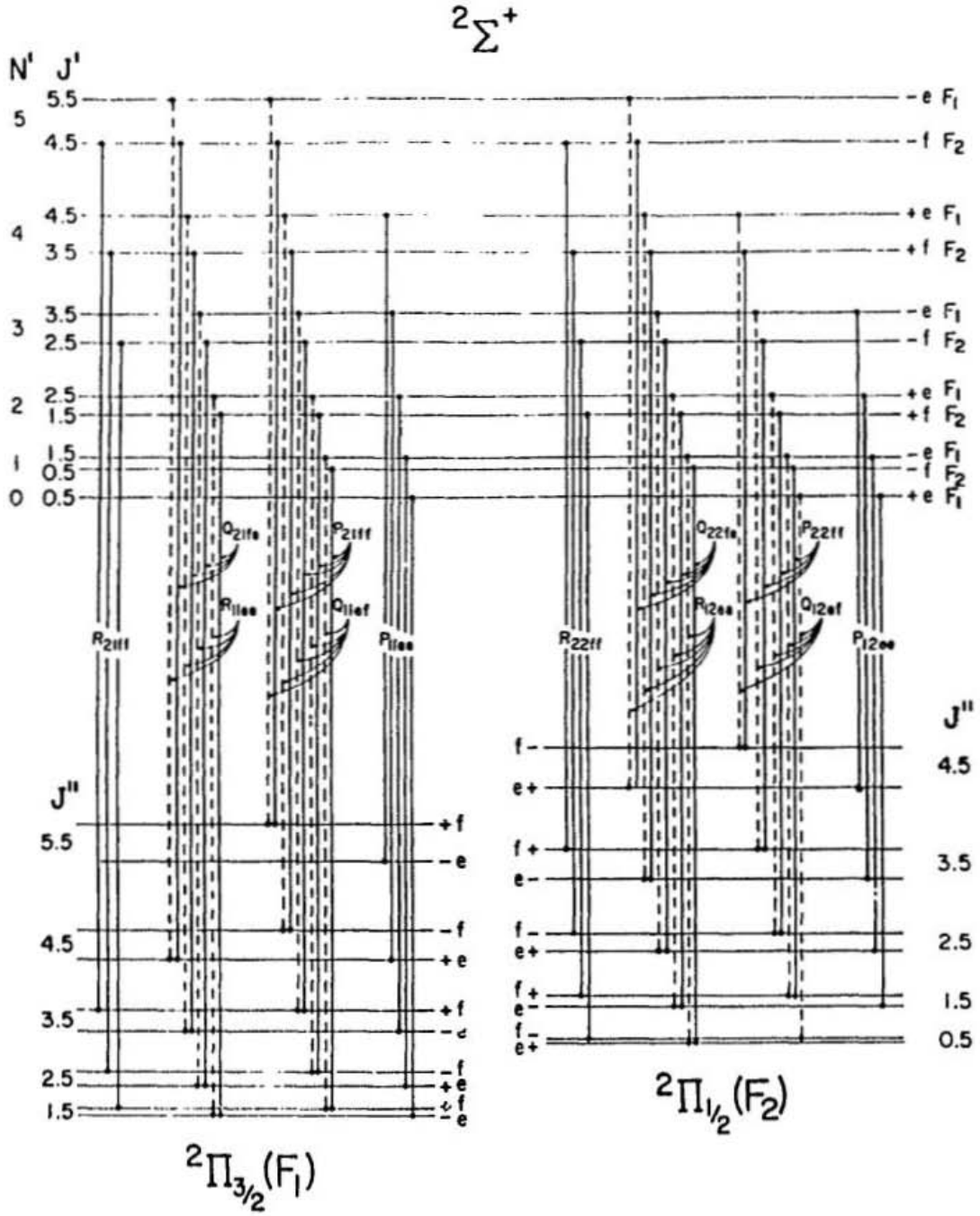

Figure 12. A schematic energy level diagram showing the first few rotational transitions of all the twelve branches of a band of a $^2\Sigma^+ - {}^2\Pi_i$ transition.

state, and 7 for each of B_v, D_v, A_v, A_{Dv}, p_v, q_v, and p_{Dv} for v = 0 and 1 levels of the $A^2\Pi_i$ state). The 20 rotational constants obtained from Merge 3 are given in Table 4.2. The values of the constants thus obtained are in good agreement with those reported by Jakubek et al. (1987) which are shown in Appendix, Table II.

4.3 The microwave data

Very precise values of the ground state molecular constants of a molecule are normally obtained from its microwave spectrum. In the present work, the microwave data reported by Sastry et al. (1981) for the v = 0 level and Bogey et al. (1983) for the v = 0, 1, and 2 levels of $X^2\Sigma^+$ of CO^+ were analyzed using the Hamiltonian of the $^2\Sigma^+$ state. The nine molecular constants (3 for each of B_v, D_v, and γ_v for v = 0, 1, and 2 levels of $X^2\Sigma^+$ state) and their standard deviations thus obtained are given in Table 4.3 in units of cm^{-1} and MHz.

4.4 Global fit

The details of the band by band analysis of the comet-tail ($A^2\Pi_i$ - $X^2\Sigma^+$), the first negative ($B^2\Sigma^+$ - $X^2\Sigma^+$) and the Baldet-Johnson ($B^2\Sigma^+$ - $A^2\Pi_i$) systems, and the microwave data of the ground state $X^2\Sigma^+$ of CO^+ are described in Sections 3.4, 4.1, 4.2, and 4.3, respectively. In this section, the details of the global fit, i.e., the grand merging of all these data are presented. As each of the electronic states B, A, and X of CO^+ is observed more than once (for example, $X^2\Sigma^+$ is

TABLE 4.2 Rotational constants[a] (in cm^{-1}) of the $B^2\Sigma^+$ and $A^2\Pi_i$ states of CO^+ obtained from the B-A system

$B^2\Sigma^+$		
Molecular constant	v = 0	v = 1
B_v	1.78458(4)	1.75456(4)
$D_v \times 10^6$	7.93(6)	8.19(6)
$\gamma_v \times 10^2$	2.122(9)	2.06(1)
$A^2\Pi_i$		
B_v	1.57957(4)	1.56016(4)
D_v	6.62(6)	6.64(7)
$-A_v$	122.051(2)	121.981(2)
$-A_{Dv} \times 10^4$	1.91(7)	0.97(11)
$p_v \times 10^2$	1.52(2)	1.45(3)
$-q_v \times 10^4$	2.3(1)	2.2(2)
$-p_{Dv} \times 10^6$	2.6(6)	4.8(1.1)

[a]Number in the parentheses is the uncertainty in the last digit and corresponds to one standard deviation.

TABLE 4.3 Rotational constants[a] (in cm^{-1}) of the $X^2\Sigma^+$ state of CO^+ obtained from the microwave data

v	B_v	$D_v \times 10^6$	$\gamma_v \times 10^4$
0	1.96746227(4)	6.317(1)	9.1056(3)
	(58983.035(1) MHz)	(0.1894(0) MHz)	(272.987(9) MHz)
1	1.9484386(2)	6.45(3)	9.0494(4)
	(58412.719(7) MHz)	(0.1935(10) MHz)	(271.296(11) MHz)
2	1.9293524(3)	6.42(4)	8.9732(5)
	(57840.530(9) MHz)	(0.1926(13) MHz)	(269.011(15) MHz)

[a]Number in parentheses is the uncertainty in the last digit and corresponds to one standard deviation.

observed in the comet-tail system, the first negative system, and the microwave spectrum) it is obvious that the rotational constants estimated for the vibrational levels of these states have multiple estimates. All these multiple estimates were merged together and a single set of constants were obtained for the X, A, and B states of CO^+.

It is convenient to combine two or more sets of separately merged parameters into a single set of parameters by a least-squares grand merge method instead of obtaining the final set of parameters through only one large single merging (see Coxon, 1978). The estimated parameters from the final grand merge are identical with those derived from the equivalent large single step merge, provided the weight matrix used in the grand merge is composed of the dispersion matrices of earlier merges but not of the variance-covariance matrices of the input parameters. In the present case, the 9 parameters (B_v, D_v, and γ_v of the v = 0, 1, and 2 levels of $X^2\Sigma^+$) obtained from the microwave spectrum of $X^2\Sigma^+$ and the 49 parameters (13 band origins, 5 for each of B_v, D_v, and γ_v of the $B^2\Sigma^+$ state, and 7 for each of B_v, D_v, and γ_v of the $X^2\Sigma^+$ state) obtained from merging (Merge 2) the bands of the first negative system were first merged together. All these 58 (9 + 49) parameters, their standard deviations, and the corresponding dispersion matrices were all used as the input parameters for Merge 4. In this merge these were reduced to 52 parameters (13 band origins, 5 for each of B_v, D_v, and γ_v of

the $B^2\Sigma^+$ state and 8 for each of B_v, D_v, and γ_v of the $X^2\Sigma^+$ state). The molecular constants obtained from Merges 1 (the A-X system), 3 (the B-A system), and 4 (combination of the B-X system and the microwave data of state X) were combined in Merge 5, in which 58 parameters from the A-X system, 23 parameters from the B-A system, and 52 parameters from the combination of the B-X system and the microwave data, thus making a total of 133 parameters, were reduced to 104 parameters (27 band origins, 8 each of B_v, D_v, and γ_v for v = 0 to 7 of $X^2\Sigma^+$, 6 each of B_v, D_v, A_v, A_{Dv}, p_v, q_v for v = 0 to 4 and v = 6 of $A^2\Pi_i$, p_{D0} and p_{D1} of $A^2\Pi_i$, 5 each of B_v, D_v, and γ_v for v = 0 to 4 of $B^2\Sigma^+$). The rotational constants thus obtained from Merge 5 for the vibrational levels of the X, A, and B states of CO^+ are listed in Table 4.4. The D_v, A_{Dv}, γ_v, p_v, and q_v values obtained in this work show a large scatter because of their smallness in their values. This can be understood from the fact that most of the experimental data is from the optical spectra. The 27 band origins obtained from Merge 5 are given in Table 4.5.

The B_v values listed in Table 4.4 were fitted to the standard spectroscopic relation,

$$B_v = B_e - \alpha_e (v + 1/2), \qquad [4.1]$$

and the equilibrium rotational constants B_e and α_e were estimated for the $X^2\Sigma^+$, $A^2\Pi_i$, and $B^2\Sigma^+$ states. The equilibrium rotational constants and their standard deviations are presented in Table 4.6. The moments of inertia I_e and the

TABLE 4.4 Rotational constants* (in cm^{-1}) of the $B^2\Sigma^+$, $A^2\Pi_i$, and $X^2\Sigma^+$ states of CO^+ from the global fit

v	B_v	$D_v \times 10^6$	$\gamma_v \times 10^3$	$-A_v$	$-A_{D_v} \times 10^4$	$p_v \times 10^2$	$q_v \times 10^4$	$-p_{D_v} \times 10^8$
				$B^2\Sigma^+$				
0	1.784782(4)	8.050(1)	19.58(5)					
1	1.754563(5)	8.226(3)	19.20(6)					
2	1.724280(9)	8.453(6)	21.01(13)					
3	1.693786(49)	8.535(26)	18.47(18)					
4	1.66409(12)	8.977(97)	9.4(3.5)					
				$A^2\Pi_i$				
0	1.579629(7)	6.752(9)	-	122.048(1)	2.75(5)	1.43(1)	-2.86(10)	2.6(6)
1	1.560316(8)	6.575(14)	-	121.989(1)	1.74(6)	1.17(2)	+0.2(1)	4.8(1.1)
2	1.540634(15)	6.829(42)	-	121.895(2)	3.77(13)	1.04(2)	+1.1(3)	-
3	1.521391(14)	6.870(23)	-	121.825(3)	1.87(16)	0.57(3)	+1.9(3)	-
4	1.501838(11)	6.337(15)	-	121.856(3)	3.42(13)	1.01(3)	-2.7(2)	-
6	1.464150(61)	13.13(30)	-	120.384(3)	5.21(38)	1.39(6)	-1.3(1.1)	-
				$X^2\Sigma^+$				
0	1.96746246(3)	6.326(1)	9.1053(3)					
1	1.94843360(9)	5.772(8)	9.0483(4)					
2	1.9293521(1)	6.374(3)	8.9730(5)					
3	1.910278(6)	6.414(3)	10.21(8)					
4	1.891097(9)	6.461(5)	12.58(12)					
5	1.87167(2)	6.404(10)	11.32(12)					
6	1.85252(1)	6.568(11)	14.11(20)					
7	1.83332(12)	6.710(95)	5.5(3.5)					

*Number in the parentheses is the uncertainty in the last digit and corresponds to one standard deviation.

TABLE 4.5 Band origins[a] (in cm^{-1}) of the three systems of CO^+ obtained from the global fit

Assignments v' - v"	Band origins
first negative system	
0-0	45631.670(3)
0-1	43449.520(3)[b]
0-2	41296.133(2)[b]
1-2	42975.322(3)
2-3	42478.744(2)
1-3	40852.196(5)
2-4	40385.754(5)
3-5	39898.797(19)
0-3	39172.795(2)
1-4	38759.363(8)
2-5	38323.175(11)
4-7	37392.187(3)
0-4	37079.881(2)
1-5	36696.777(10)
2-6	36291.052(2)
comet-tail system	
6-0	29212.896(6)
4-0	26384.761(2)
3-0	24930.349(2)
2-0	23449.261(2)
1-0	21941.207(1)
2-1	21265.235(1)
1-1	19757.589(1)
0-1	18222.298(1)
2-3	16988.481(1)
0-2	16068.575(1)
0-3	13945.464(2)
0-4	11852.563(2)[b]
Baldet-Johnson system	
1-0	26906.986(1)
0-0	25227.587(1)
0-1	23692.359(1)

[a]Number in the parentheses is the uncertainty in the last digit and corresponds to one standard deviation.

[b]The band origins are obtained from the band by band analysis.

TABLE 4.6 Equilibrium molecular constants[a] (in cm^{-1}) of the $X^2\Sigma^+$, $A^2\Pi_i$, and $B^2\Sigma^+$ states of CO^+

Molecular constant	$X^2\Sigma^+$	$A^2\Pi_i$	$B^2\Sigma^+$
T_e	0.0	20731.790(2)	45876.797(3)
ω_e	2214.088(2)	1562.075(2)	1734.447(8)
$\omega_e x_e$	15.0929(8)	13.5364(9)	28.131(5)
$\omega_e y_e$	-0.00767(8)	0.01028(9)	0.3674(7)
B_e	1.97698785(5)	1.589444(7)	1.799980(4)
α_e	0.01904853(5)	0.019461(3)	0.030146(3)
$D_e \times 10^6$	6.305[b]	6.583[b]	7.754[b]
r_e(Å)	1.11521840(1)	1.243768(3)	1.168767(1)
$I_e(\mu cm^2) \times 10^{39}$	1.41595200(1)	1.761194(3)	1.555195(1)

[a]Number in the parentheses is the uncertainty in the last digit and corresponds to one standard deviation.

[b]Calculated from the expression $D_e = 4B_e^3/\omega_e^2$.

equilibrium internuclear distances r_e calculated from the corresponding B_e values are also presented in the same table.

All the band origins given in Table 4.5 were fitted together to the expression

$$\nu_{v',v''} = \nu_e + \omega'_e(v'+1/2) - \omega'_e x'_e(v'+1/2)^2 + \omega'_e y'_e(v'+1/2)^3 - \omega''_e(v''+1/2) + \omega''_e x''_e(v''+1/2)^2 - \omega''_e y''_e(v''+1/2)^3. \quad [4.2]$$

The vibrational constants ω_e, $\omega_e x_e$, and $\omega_e y_e$ of all the three states and the system origins of the A-X and B-X systems were obtained simultaneously from this fit. All these constants, along with their standard deviations, are listed in Table 4.6. The term values of T_e of the $A^2\Pi_i$ and $B^2\Sigma^+$ states listed in this table, are the same as the system origins of the A-X and B-X systems respectively. The equilibrium centrifugal stretching constants D_e were calculated for the X, A, and B states from the expression,

$$D_e = \frac{4B_e^3}{\omega_e^2}, \quad [4.3]$$

using the corresponding B_e and ω_e values and are listed in the same table. The vibrational term values of the vibrational levels of the states X, A, and B relative to the v = 0 level of X were obtained from all the band origins listed in Table 4.5 and are listed in Table 4.7 along with their standard deviations. The position of the v = 0 level of state X relative to its potential minima is calculated using its vibrational constants and is found to be 1103.270 cm^{-1}. It is appropriate to comment on the accuracy obtained in this work.

TABLE 4.7 Vibrational term values[a] (in cm^{-1}) of the $X^2\Sigma^+$, $A^2\Pi_i$ and $B^2\Sigma^+$ states of CO^+

v	$X^2\Sigma^+$	$A^2\Pi_i$	$B^2\Sigma^+$
0	0.0[b]	20406.155(1)	45633.765(1)
1	2183.808(1)	21941.246(1)	47313.133(2)
2	4337.601(1)	23449.120(1)	48939.436(3)
3	6460.659(1)	24930.349(2)	50514.973(22)
4	8553.882(2)	26384.761(2)	52042.365[c]
5	10616.203(10)	27812.599[c]	
6	12648.384(4)	29212.896(2)	
7	14650.179[c]		

[a]Number in the parentheses is the uncertainty in the last digit and corresponds to one standard deviation.

[b]The term values are expressed relative to the v = 0 level of the $X^2\Sigma^+$ state, which is at 1103.270 cm^{-1} above the minimum of its potential energy curve.

[c]This term value is calculated from the expression $T_e+G(v)$ - 1103.270 cm^{-1}.

For example, the B_o values of the ground state of CO$^+$ are 1.96623(3), 1.96723(2), and 1.96746227(4) obtained from the A-X system, the B-X system, and the microwave data respectively. The final value reported from the global fit in Table 4.4 is 1.96746246(3). Even though the values obtained from the A-X and B-X systems are less accurate than the value obtained from the microwave data (Sastry et al. 1981 and Bogey et al. 1983), the inclusion of the latter has helped to obtain more precise value from the global fit, than from the optical data. It can be also seen from Tables 4.1 and 4.2 that the B_v values obtained from the data of Misra et al. (1987) and Jakubek et al. (1987) are accurate up to 5th decimal place whereas the corresponding values obtained from the global fit in the present work are accurate up to 6th decimal place. Thus the molecular constants obtained from the global fit are more precise at least by one order of magnitude than the values existing in the literature.

REFERENCES

Abell, G. O., 1975, "Exploration of the Universe", 3rd ed., Holt, Rinehart and Winston, New York.

Albritton, D. L., Schmeltekopf, A. L., and Zare, R. N., 1977, J. Mol. Spectrosc., 67, 132-156.

Amiot, C., Maillard, J. P., and Chauville, J., 1981, J. Mol. Spectrosc., 87, 196-218.

Asundi, R. K., Dhumwad, R. K., and Patwardhan, A. B., 1970, J. Mol. Spectrosc., 34, 528-532.

Baldet, F., 1924, Compt. Rend., 178, 1525-1527.

Baldet, F., 1925a, Compt. Rend. 180, 271-273.

Baldet, F., 1925b, Compt. Rend. 180, 820-822.

Birge, R. T., 1925, Nature, 116, 170-171L.

Biskamp, H., 1933, Z. Physik, 86, 33-41.

Blackburn, C. M., 1925, Proc. Natl. Acad. Sci., 11, 28-34.

Bogey, M., Demuynck, C., and Destombes, J. L., 1982, Mol. Phys., 46, 679-681.

Bogey, M., Demuynck, C., and Destombes, J. L., 1983, J. Chem. Phys., 79, 4704-4707.

Brown, R. D., Dittman, R. G., McGilvery, D. C., and Godfrey, P. D., 1983, J. Mol. Spectrosc., 101, 61-70.

Brown, R. D., Dittman, R. G., and McGilvery, D. C., 1984, J. Mol. Spectrosc., 104, 337-342.

Brown, J. M., Hougen, J. T., Huber, K. P., Johns, J. W. C., Kopp, I., Lefebvre-Brion, H., Merer, A. J., Ramsay, D. A., Rostas, J., and Zare, R. N., 1975, J. Mol. Spectrosc., 55, 500-503.

Brown, J. M., Colbourn, E. A., Watson, J. K. G., and Wayne, F. D., 1979, J. Mol. Spectrosc., 74, 294-318.

Bulthuis, H., 1934, Physica, 1, 873-880.

Bulthuis, H., 1935, Proc. Acad. Sci. Amsterdam, 38, 604-617.

Čonkić, L., Janjić, J. D., Pešić, D. S., Rakotoarijimy, D., Vujisić, B. R., and Weniger, S., 1978, Astrophys. J., 226, 1162-1170.

Coster, D., Brons, H. H., and Bulthuis, H., 1932, Z. Physik, 79, 787-822.

Coxon, J. A., and Foster, S. C., 1982, J. Mol. Spectrosc., 93, 117-130.

Coxon, J. A., 1978, J. Mol. Spectrosc., 72, 252-263.

Crosswhite, H. M., 1975, J. Res. Natl. Bur. Stds., A Phys. and Chem., 79A, 17-69.

Crosswhite, H. M., 1958, John Hopkins Spectroscopic Report No. 13.

Dhumwad, R. K., Patwardhan, A. B., and Kulkarni, V. T., 1979, J. Mol. Spectrosc., 78, 341-343.

Dixon, T. A., and Woods, R. C., 1975, Phys. Rev. Lett., 34, 61-63.

Edlen, B., 1953, J. Opt. Soc. Amer., 43, 339-344.

Fowler, A., 1910, Monthly Notices Roy. Astron. Soc., 70, 484-496.

Fowler, A., 1909, Monthly Notices Roy. Astron. Soc., 70, 176-182.

Gagnaire, H., and Goure, J. P., 1976, Can. J. Phys., 54, 2111-2117.

Herzberg, G., 1950, "Molecular Spectra and Molecular Structure", Vol. I, "Spectra of Diatomic Molecules", 2nd ed., D. Van Nostrand Company, Inc., New York.

Herzberg, G., Lew, H., Sloan, J. J., and Watson, J. K. G., 1981, Can. J. Phys., 59, 428-440.

Huber, K. P., and Herzberg, G., 1979, "Molecular Spectra and Molecular Structure", Vol. IV, "Constants of Diatomic Molecules", Van Nostrand Reinhold Company, New York.

Jakubek, Z., Kepa, R., Para, A., and Rytel, M., 1987, Can. J. Phys., 65, 94-100.

Johnson, R. C., 1925, Proc. Roy. Soc. (London), Ser. A, 108, 343-355.

Katayama, D. H., and Welsh, J. A., 1981, J. Chem. Phys., 75, 4224-4230.

Kopp, I., and Hougen, J. T., 1967, Can. J. Phys., 45, 2581-2596.

Krupenie, P. H., 1966, "The Band Spectrum of Carbon Monoxide", National Standard Reference Data Series, Natl. Bur. Stand., Vol. 5.

Lefebvre-Brion, H., Moser, C. M., and Nesbet, R. K., 1964, J. Mol. Spectrosc., 13, 418-429.

Marchand, J., D'Incan, J., and Janin, J., 1969, Spectrochim. Acta, 25A, 605-609.

Misra, P., Ferguson, D. W., Rao, K. N., Williams Jr. E., and Mathews, C. W., 1987, J. Mol. Spectrosc., 125, 54-65.

Mulliken, R. S., 1932, Rev. Mod. Phys., 4, 1-86.

Piltch, N. D., Szanto, P. G., Anderson, T. G., Gudeman, C. S., Dixon, T. A., and Woods, R. C., 1982, J. Chem. Phys., 76, 3385-3388.

Pluvinel, A. B., and Baldet, F., 1909, Compt. Rend., 148, 759-762.

Pluvinel, A. B., and Baldet, F., 1911, Astrophys. J., 34, 89-104.

Prasad, C. V. V., and Reddy, S. P., 1988, J. Mol. Spectrosc., 130, 62-68.

Prasad, C. V. V., and Reddy, S. P., 1989, J. Chem. Phys., 90, 3010-3014.

Prasad, C. V. V., and Reddy, S. P., 1990, J. Chem. Phys., (in press).

Rao, K. N., 1950a, Astrophys. J., 111, 306-313.

Rao, K. N., 1950b, Astrophys. J., 111, 50-59.

Rao, K. N., and Sarma, K. S., 1953, Mem. Soc. Roy. Sci. Liege Collect., 13, 181-186.

Reddy, S. P., and Prasad, C. V. V., 1989a, J. Chem. Phys., 91, 1972-1977.

Reddy, S. P., and Prasad, C. V. V., 1989b, J. Phys. E. Sci. Instrum., 22, 306-308.

Sastry, K. V. L. N., Helminger, P., Herbst, E., and DeLucia, F. C., 1981, Astrophys. J., 250, L91-L92.

Schmid, R. F., 1932, Phys. Rev., 42, 182-188.

Schmid, R., and Gerö, L., 1933, Z. Physik, 86, 297-313.

Van den Heuvel, F. C., Meerts, W. L., and Dymanus, A., 1982, Chem. Phys. Lett., 92, 215.

Vujisić, B. R., Pešić, D. S., Weniger, S., and Rakotoarijimy, D., 1980, Indian. J. Pure and Appl. Phys., 18, 370-372.

Vujisić, B. R., and Pešić D. S., 1988, J. Mol. Spectrosc., 128, 334-349.

Woods, L. H., 1943, Phys. Rev., 63, 431-432.

Wurm, K., 1943, Vierteljahresschr. d. Astr. Ges., 78, 18.

APPENDIX

In this Appendix, the molecular constants of CO' obtained from the first negative system by Misra et al. (1987), Baldet-Johnson system by Jakubek et al. (1987), and the microwave data of the v = 0,1 and 2 levels of $X^2\Sigma^+$ state by Sastry et al. (1981) and Bogey et al. (1982) are presented in Table I, II, and III respectively. The differences $|\gamma'_v - \gamma''_v|$ for the $B^2\Sigma^+ - X^2\Sigma^+$ system obtained in the present work and those available in the literature are compared in Table IV.

TABLE I Rotational constants[a] (in cm^{-1}) of the $B^2\Sigma^+$ and $X^2\Sigma^+$ states of CO^+ by Misra et al. (1987).

v	B_v	$D_v \times 10^6$	$\gamma_v \times 10^2$
	$B^2\Sigma^+$		
0	1.784787(45)	8.078(37)	1.664(66)
1	1.75466(10)	8.274(58)	1.51(13)
2	1.72433(11)	8.496(71)	1.23(14)
3	1.69393(20)	8.63(13)	1.35(22)
	$X^2\Sigma^+$		
0	1.9674656(31)	6.354(38)	0.91051(89)
1	1.9484388(43)	6.344(47)	0.9048(12)
2	1.929479(63)	6.437(41)	0.846(25)
3	1.910331(97)	6.464(58)	0.97(12)
4	1.89107(11)	6.468(70)	0.49(16)
5	1.87176(13)	6.466(84)	0.63(17)
6	1.85255(17)	6.59(12)	0.49(20)

[a]Number in the parentheses is the uncertainty in the last digit and corresponds to one standard deviation.

TABLE III Rotational constants[a] (in cm^{-1}) of the $X^2\Sigma^+$ state of CO^+ obtained from the microwave data

v	B_v	$D_v \times 10^6$	$\gamma_v \times 10^3$
0	1.9674624(4)[b]	6.32(2)[b]	9.107(2)[c]
	(58983.040(12) MHz)	(0.1895(5) MHz)	(273.01(5) MHz)
1	1.948439(1)[c]	6.45(3)[d]	9.049(4)[c]
	(58412.72(4) MHz)	(0.194(1) MHz)	(271.27(11) MHz)
2	1.929347(4)[c]	6.42(2)[d]	8.991(8)[c]
	(57840.37(13) MHz)	(0.193(1) MHz)	(269.53(23) MHz)

[a]Number in parentheses is the uncertainty in the last digit and corresponds to one standard deviation.

[b]Sastry et al. (1981).

[c]Bogey et al. (1982).

[d]Calculated in the present work from the experimental data of Bogey et al. (1983).

TABLE II Rotational constants[a] (in cm^{-1}) of the $B^2\Sigma^+$ and $A^2\Pi_i$ states of CO^+ by Jakubek et al. (1987)

$B^2\Sigma^+$		
Molecular constant	v = 0	v = 1
B_v	1.784564(54)	1.754520(56)
$D_v \times 10^6$	7.941(78)	8.153(78)
$\gamma_v \times 10^2$	2.116(11)	2.065(15)
T_v	25227.6135(24)	26906.9837(29)
$A_2\Pi_i$		
B_v	1.579539(54)	1.560115(58)
$D_v \times 10^6$	6.602(76)	6.595(86)
$-A_v$	122.0507(28)	121.9856(32)
$-A_{Dv} \times 10^4$	1.927(97)	1.051(136)
$P_v \times 10^2$	1.531(32)	1.412(43)
$-q_v \times 10^4$	2.27(16)	2.47(26)
$-p_{Dv} \times 10^6$	3.10(77)	2.87(123)
T_v	0	1535.0585(31)

[a]The number in the parentheses indicates the uncertainty in the last digit and correspond to one standard deviation.

TABLE IV Comparison of the values of $|\gamma'_v - \gamma''_v|$ (in cm^{-1}) obtained in the present work with the previous values.

(v',v")	$\|\gamma'_v - \gamma''_v\|$		
	Woods (1943)	Rao (1950a)	Present work
(0,1)	0.0180	0.009	0.0092
(0,2)	0.0159	0.008	0.0092
(0,3)	0.0153	0.010	0.0093
(1,2)	0.0172	0.009	0.0092
(1,3)	0.0158	0.008	0.0092
(1,4)	0.0150	0.010	0.0067
(1,5)	0.0159	0.009	0.0079
(2,4)	0.0149	0.009	0.0085
(2,5)	0.0153	0.009	0.0096
(2,6)	0.0150	0.008	0.0069
(3,5)	0.0153	0.007	0.0071